LATE QUATERNARY STUDIES ON CLIMATE VARIABILITY IN INDIAN SECTOR OF SOUTHERN OCEAN USING DIATOMS

A Thesis

submitted to the Goa University for the Award of the Degree

of

DOCTOR OF PHILOSOPHY

in

Marine Sciences

by

Abhilash Nair

Research guide

Dr. Rahul Mohan

National Centre for Polar and Ocean Research

Vasco-da-Gama, Goa - 403804, India.

Co-guide

Dr. Thamban Meloth

National Centre for Polar and Ocean Research

January 2019

DEDICATED TO MY FAMILY AND FRIENDS

STATEMENT

As required under the University Ordinance OB-9A, I hereby state that the current thesis titled "**LATE QUATERNARY STUDIES ON CLIMATE VARIABILITY IN INDIAN SECTOR OF SOUTHERN OCEAN USING DIATOMS**" is my original contribution and the same has not been submitted on any previous occasion. To the best of my knowledge, the present study is the first comprehensive work of its kind from the area mentioned. The literature related to the problem investigated has been cited. Due acknowledgements have been made wherever facilities and suggestions have been availed of.

January, 2019

ABHILASH NAIR

CERTIFICATE

As required under the University Ordinance OB-9A, it is certified that the thesis titled "**LATE QUATERNARY STUDIES ON CLIMATE VARIABILITY IN INDIAN SECTOR OF SOUTHERN OCEAN USING DIATOMS**", submitted by **ABHILASH NAIR** for the award of the degree of Doctor of Philosophy in Marine Sciences, Goa University, is based on original studies carried-out by him under my supervision. The thesis or any part of thesis has not been previously submitted for any other degree or diploma in any university or institution.

Dr. RAHUL MOHAN **Dr. THAMBAN MELOTH**

(Guide) **(Co-guide)**

ACKNOWLEDGEMENTS

To begin with, I would like to thank my research guide and supervisor Dr. Rahul Mohan, whose subject knowledge, understanding, and patience, played a vital part in my PhD research. His efficient guidance assisted me in research and in writing my thesis. I wish to express my sincere gratitude to him for encouraging my work with lots of valuable discussions and suggestions and giving me lots of opportunities to present my work and getting trained in the relevant scientific field.

I also thank Dr. Thamban Meloth for being my co-guide and guiding me and giving valuable suggestions during my research tenure.

I am grateful and thankful to Dr. M. Ravichandran (Director), Dr. S. Rajan (Ex-director) and Dr. Rasik Ravindra (Ex-director), ESSO-National Centre for Polar & Ocean Research, Ministry of Earth Sciences, Govt. of India, for giving me the research fellowships, support and facilitating my thesis work.

I also like to acknowledge Dr. B. Nagender Nath, subject expert, for duly assessing my work progress and providing valuable suggestions. Also, my sincere thanks goes out to Prof. G.N. Nayak, Prof. C. U. Rivonker and other Faculty Research Committee members for examining my research progress and guiding me all through.

I also wish to thank Manoj M.C. for supporting and providing important suggestions in field of Southern Ocean Paleoceanography, which helped me immensely during the course of my study.

I'm extremely grateful to Dr. Xavier Crosta, University of Bordeaux, France for guiding, training, and helping me out with the dataset.

A Special mention goes out to Sadhguru Jaggi Vasudev, Isha Yoga Centre, Coimbatore, India for getting me introduced to yoga and helping me develop integrity and focus in life. I'm immensely indebted to you.

Various other friends and colleagues supported my study scientifically and non-scientifically, and I honestly thank all of them for their generous assistance. To start with, I am thankful to all my lab mates for their help and support during my thesis work. I thank Mahesh Badanal and Anish Warrier for guiding me with suggestions both on and off research field which helped me greatly to carry out this work. I'm also grateful to Ravi

Naik for providing his valuable suggestions during my research tenure which assisted me in carrying out my PhD work. A big thanks to *Ms. Sahina Gazi for helping me carry out the analysis using Scanning electron microscope. I thank Shramik Patil and Suhas Shetye for helping me in various ways in completing the PhD work. And thanks to Nibedita, Nuruzamma, Pallavi, Pooja, Shubam, Siddesh, Kartik, Kalpana, Vailancy, Hari, Cheryl, Saalim, Michelle, Swati, Sweta and Ankita for helping and supporting me.*

Finally, thanks to my family for their support, love, faith and encouragement during all these years, this work is dedicated to you all.

Abhilash Nair

TABLE OF CONTENTS

FIGURES AND TABLES

Chapter 1. Introduction

Chapter 2. Materials and methods

Chapter 3. Annotated index of key diatom species

Chapter 4. Variability in diatom abundance and valve size

Chapter 5. Comparison of Southern Ocean data with other climatic records

PREFACE

The present study aims to document the past latitudinal shifts of Southern Ocean sea ice and frontal systems and their potential impact on different climate systems. The introductory chapter describes the importance and significance of the proposed work in the field of Southern Ocean paleoceanography. Here few vital problems /questions related to Southern Ocean's role in a global climate variability along with the need for paleoceanoraphy research is highlighted. Additionally, emphasis is laid on the robustness of diatoms as a proxy to reconstruct paleo sea surface temperature and sea ice variability in Southern Ocean in order to study their role in oceanic circulations as well as carbon dioxide uptake. Further a brief introduction on Indian sector of Southern Ocean is incorporated along with its regional intricacies and followed by the need to take up the present study. This is then followed by the description of regional settings and methodology adopted to achieve the objectives. This study is based on quantitative sea-surface temperature (SST) and sea ice reconstructions using diatom along with diatom absolute abundances and diatom biometry from two sediment cores located at sub-Antarctic front (SAF) and Antarctic Polar front (APF) in the southwest Indian sector of the Southern Ocean. The next chapter highlights the key taxonomic details and distribution of key diatom groups/species from Southern Ocean. The following chapters (chapter 4-6) of the thesis provides insight into the glacial-interglacial variation of different diatom-based records from the studied region and their comparison with other climatic records. Our study suggests the presence of the mean winter sea ice limit at around the ice-free modern Antarctic polar front location (~49°S) during the Marine isotopic stage 2 and 4 and episodic/unconsolidated winter sea ice as north as ~43°S during the last glacial maxima, when SST were lowest. Lower than present day SST along with higher diatom productivity and larger mean sizes of *F. kerguelensis* and *T. lentiginosa* recorded at the northern core site during the glacial periods suggest a northward shift of the APF. A decrease in glacial diatom productivity and sizes at the southern core site highlights stratified POOZ surface waters in response to longer sea ice presence. Further this study documents and reviews the past complex interaction between the Southern Hemisphere high-latitude (Southern Ocean SST, sea ice and

Antarctic temperatures), Southern Indian Ocean subtropics and Asian summer monsoon.

Chapter 1

Introduction

1.1. Motivation

The Quaternary period spans about last two and half million years of Earth's history (Cohen et al, 2013) and is well known for the period of ice ages. The late Quaternary is characterised by repeated cycles of cold-warm climatic oscillations as Earth alternated between glacial and interglacial periods. Such glacial-interglacial climate changes were primarily controlled by cyclic variation in insolation. The "pacemaker of the ice ages" as it is known, is driven by variations in Earth's orbital elements, including the path around the sun, the tilt of the earth's axis (obliquity) and precession of the equinoxes (Hays et al., 1976; Epica members, 2004; Lisiecki and Raymo, 2005).

To improve our understanding on the late Quaternary climate, the time interval covering at least the last glacial period needs to be studied i.e. the late Pleistocene to Holocene time interval. During this time span, earth had undergone transition from warm interglacial period i.e. Marine isotopic stage (MIS) 5 to cold interval (MIS 4 and LGM) and returning back to present warm period (interglacial period), also including several other abrupt climatic events during this transition. The mechanisms governing the climate variability during this time interval is vital for it may correspond to the longer past earth history.

Overlaid on the long term glacial-interglacial cycles were much shorter periods of abrupt climate shifts, probably due to the complex ocean-atmosphere interaction. Numerous such abrupt events during the last glacial period/cycle i.e. between 110.8 and 11.7 ka BP (Martinson et al., 1987; Lowe et al., 2008b) were observed in both hemispheres, where the Antarctic warming phase (Antarctic isotope maximum) corresponds to a cold stadial (Heinrich events) in Greenland (Epica members, 2006). Water isotope records from the stacks of Greenland and Antarctica exemplify a seesaw pattern with the Greenland warming being concomitant with the beginning of the Antarctica cooling at the Antarctic Isotopic Maximum (Blunier and Brook, 2001). During the last glacial cycle, it is also known that the timings of the maximum extent of the mountain glaciers and continental ice sheets differed, often well before global Last glacial Maximum (LGM) (Hughes et al., 2013). Hence the exact mechanisms of the climate variability, extent and

chronology of glaciation during the late Quaternary will be under the scanner of active research and will continue to challenge the scientists in the future.

The global temperatures and sea level (ca. 120-130m lower than present) during LGM were significantly lower than the present (Yokoyama et al., 2000; Jansen et al., 2007; Margo members, 2009). Vast regions of northern hemisphere high latitude and higher elevations of lower latitude were covered by continental ice; the East and West Antarctica, South America also contained significantly greater ice volume than present day scenario (Anderson et al., 2002; Clark et al., 2009; Hein et al., 2010). The sea ice cover during LGM was significantly extended (latitudinally) in northern as well as southern hemispheres (Gersonde et al., 2005; de Vernal et al., 2006). LGM was also a period of strengthened southern hemisphere westerlies and relatively dustier conditions, which possibly increased marine biological productivity (Maher et al., 2010; Martinez-Garcia et al., 2011). The duration between the LGM termination and Holocene experienced dissimilar timing of warming between northern and southern hemispheres. Such post glacial warming may be linked to freshening of the ocean or latitudinal shift in the westerlies from southern hemisphere, and consequent variations in ocean circulation (Bianchi and Gersonde, 2004; McManus et al., 2004; Epica members, 2006; Denton et al., 2010). Holocene is presumably considered to be relatively a steady interglacial period, however, large time and space bound climate variations are extensively documented in this period (Mayewski et al., 2004; Jansen et al., 2007). Even though the break through made in last few decades in intensively studying the Last Glacial period to Holocene climate dynamics, the knowledge from the southern hemisphere high latitudes is quite inadequate. In southern high latitude, Antarctic ice cores are primary archives providing high resolution records, oceanic records are limited as compared to the surplus records from northern hemisphere, tropical and sub-tropical regions, this restrict the validation of the oceanic processes in climate feedback and forcing.

Primary hurdle in inferring the climate signals from Southern Ocean sediments is in to generate core stratigraphy. The measurement of oxygen isotope data or radiocarbon dating using carbonate microfossils is hampered, given the amount of carbonate preserved in the sediments south of the Antarctic Polar Front. Instead, sedimentary organic matters are radiocarbon dated (Domack et al., 2001;

Bianchi and Gersonde, 2004; Denis et al., 2009; Hillenbrand et al., 2009). However, further complications in the dependability of the core age model is created by the uncertainty in Southern Ocean carbon reservoir effect (Sikes et al., 2000; van Beek et al., 2002) which may be linked to the history of Southern Ocean ventilation (Skinner et al., 2010). Accordingly, age core models are established using alternative proxies like radiolarian (Abelmann and Gersonde, 1991; Brathauer et al., 2001), diatom (Burckle and Burak, 1988; Kaczmarska et al., 1993; Zielinski et al., 2002; Zielinski and Gersonde, 2002), magnetic susceptibility record (Schmieder, 2004; Pugh et al., 2009), and geomagnetic paleointensity (Stoner et al., 2002; Lund et al., 2006; Macri et al., 2006; Channell et al., 2009). But, these proxies have certain limitations in terms of accuracy or location constraints or sedimentary settings. The understanding about the validation of these proxies and their relation in response to changes in the Southern Ocean processes associated with climate change is not clear.

1.2. Background Information

1.2.1. The Southern Ocean

The opening of the Tasmania-Antarctic and Drake Passages during the Eocene-Oligocene Boundary led to the formation of the Southern Ocean (Lawver and Gahagan, 2003; Scher and Martin, 2006). It is the formation of the Antarctic Circumpolar Current (ACC) instigated by the opening of the deep water pass ways led to the separation of Antarctica. This led to the decrease in the north-south heat transport and induced glaciation since Eocene-Oligocene boundary (Zachos et al., 2001; Barker and Thomas, 2004; Mackensen, 2004; Barker et al., 2007). A pioneering study by Jenkins, (1974) described the onset of a proto-ACC on the basis of an eastward spread of a planktonic foraminifer *Guembelitria stavensis* into the south-west Pacific from a region south of Australia, using a mixture of onshore and offshore data. The Southern Ocean is the sole connecting link for the Atlantic, Pacific and Indian Oceans, thus forming a junction for the exchange of water mass and heat for the world oceans, hence it is a vital component of the thermohaline circulation (Fig.1).

The ACC is one of the crucial component of the Southern Ocean and is globally the major ocean current. It accounts for ~130 Sv (106 m3/s) transport passing via Drake Passage (Whitworth and Peterson, 1985; Cunningham et al., 2003), circum-navigating the Antarctica having length ~ 24,000 km (Olbers, et al., 2004). The southern hemisphere westerly winds drive the ACC and, in maximum places, it flows deeper, close to the sea bed (Orsi et al., 1995; Barker and Thomas, 2004). Series of oceanic fronts, classified based on the water properties such as temperature, salinity and density are present within the ACC. The major fronts from north to the south are Subtropical Front (STF), Sub-Antarctic Front (SAF), Antarctic Polar Front (APF) and Southern ACC Front (Orsi et al., 1995). The presence of this oceanic fronts allow for the zonal division of the Southern Ocean in to Sub-Antarctic Zone (SAZ) which is bordered by STF and SAF; Polar Frontal Zone (PFZ) is bounded by SAF and APF; and the Antarctic Zone (AZ) by PF and the Antarctic continent (Belkin and Gordon, 1996).

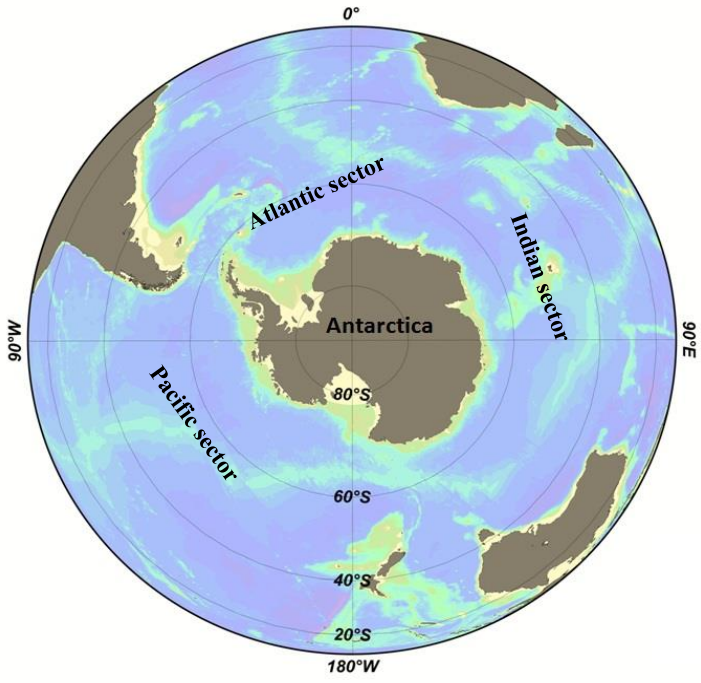

Fig.1. Southern Ocean Map comprising of Indian, Atlantic and Pacific sector.

The APF is the essential front amongst the ACC fronts, since it is the site which is called as the Antarctic Convergence where Antarctic surface waters

flowing northward downwells quickly below Sub-Antarctic waters (Orsi et al., 1995). The sea surface temperature (SST) across the APF, varies ~1.35°C over an area < 60 km (Moore et al., 1997). Currently the ACC core occurs at ~ 4°C isotherm of summer SST at the APF (Olbers et al., 2004). Both the SAF and APF constitutes 40-70% of ACC transport (Gille, 1994), and the average pass of SAF and APF are bathymetry controlled (Gille, 1994; Moore et al., 1997; Moore et al., 1999; Dong et al., 2006). Governed by bathymetry there is a spatial difference in the mean position of the APF, in the Atlantic and Indian sectors it is positioned roughly at 45-50°S and located to the north relative to the Pacific sector (ca. 60-65°S) (Orsi et al., 1995). In terms of paleoscience perspective, glacial-interglacial fluctuation in the latitudinal mean position of the APF, is probably linked to latitudinal shifts in the wind field and sea ice (Moore et al., 1997; 1999; Bryden and Cunningham, 2003; Barker and Thomas, 2004; Dong et al., 2006).

Apart from ACC, sea ice distribution is an important feature of the Southern Ocean in terms of spatial and seasonal variation. Antarctic sea ice has a maximum coverage in austral winter, spanning an area of ~18.3 $\times 10^6$ km^2 during September, sea ice cover reduces to its minimum in austral summer around February having an area ~3×10^6 km^2 specifically in the Bellingshausen Sea, western Weddell Sea, , Amundsen Sea and portions of the Ross Sea and the Indian sector (Comiso, 2010). Sea ice is an important parameter of the climate system that influences energy and gas balances, and deep ocean convection (Budd, 1975; Ackley, 1980). During sea ice formation, vertical convection and/or bottom water formation is initiated through brine rejection. In contrast, the sea ice melting forms a low salinity surface water lens that causes stratification of above water column and assists in increasing the biological productivity by providing stability in the surface water. Sea ice melting also leads to iron fertilization of high latitude Southern Ocean through the release of sea ice laden dust into the surrounding waters, thereby enhancing the carbon export to the ocean bottom (Abelmann et al., 2006). Hence it is obvious that from sea ice to open ocean regime the sedimentary composition is bound to vary which is thus reflected in the sediment core lithology on a glacial-interglacial time scale.

The modern Southern Ocean lithology shown in Fig. 2 (modified after Diekmann, 2007) represents a revised form of the previous compilation by Cooke (1978) (in Burckle et al., 1982) with reference to opal data and maps from previous publications (Burckle and Cirilli, 1987; McCoy, 1991; Zielinski and Gersonde, 1997; Bareille et al., 1998; Pudsey and Howe, 1998; Dezileau et al., 2000; Chase et al., 2003; Geibert et al., 2005). It must be remembered that the illustration of the lithofacies (Fig. 2) should be perceived in a qualitative manner, because it is basically generalized and based on diverse approaches (core descriptions, smear slides, chemical component analyses, X-ray diffraction, and accumulation rates). The continental margin of Antarctica is plastered by glacial-marine and hemipelagic siliciclastics (Anderson, 1999). Submarine highs and mounds, like Maud Rise and the Kerguelen Plateau are primarily roofed by high abundances of foraminifera and diatoms. Further offshore, the deep basins (Weddell and Enderby) encircling Antarctica comprises of deep-sea clays. The northern limit of seasonal sea-ice extent is strongly affected by relatively high surface water productivity due to the increased light availability, the export of biosiliceous and calcareous debris to the sediment. The location of the APF in this context plays a significant role, as it is an ecological and physical water-mass boundary, demarking cold and silicate-replete waters to the south and warmer and saline waters to the north. Calcareous oozes dominate the sediment north of the APF, whereas sediment south of the APF is characterised by diatomaceous oozes forming the Circum-Antarctic Opal Belt of sediment beneath the permanently open-ocean zone (Burckle and Cirilli, 1987). The prevalence of the opal belt is not completely the consequence of relatively high primary biological productivity; besides, it depicts the high preservation of biogenic opal in that region (Schlu¨ ter et al., 1998; Pondaven et al., 2000).

The Southern Ocean plays a vital role as driver of and responder to the global climate by playing its part in global carbon cycle, physical oceanography and the marine ecosystem. The essential role of Southern Ocean is believed to reflect its leverage on the global efficiency of the biological pump, in which the carbon is sequestrated in ocean interior through production, sinking, and deep remineralisation of organic matter, thereby lowering atmospheric CO_2 (Sigman and Boyle, 2000; Kohfeld et al., 2005; Jaccard et al., 2013). During glacial times the efficient export of carbon to the deeper depths of Southern Ocean by biological

pump (Kohfeld et al., 2005; Abelmann et al., 2006) is believed to have lowered the atmospheric CO_2 and heavily stratified surface waters prevented the ventilation of CO_2 from the bottom deep waters (Stephens and Keeling, 2000; Sigman et al., 2004; Hillenbrand and Cortese, 2006; Bouttes et al., 2009). In addition, the glacial CO_2 reduction associated with these mechanisms would have been amplified by iron fertilization of the Sub-Antarctic zone of the Southern Ocean (Kumar et al., 1995; Martinez-Garcia et al., 2011). Contrastingly, during the post glacial warming, prevalence of vertical mixing in the Southern Ocean might have probably released the sequestered CO_2 back into the atmosphere, thereby possibly intensifying the warming mechanism (Anderson et al., 2009; 2010).

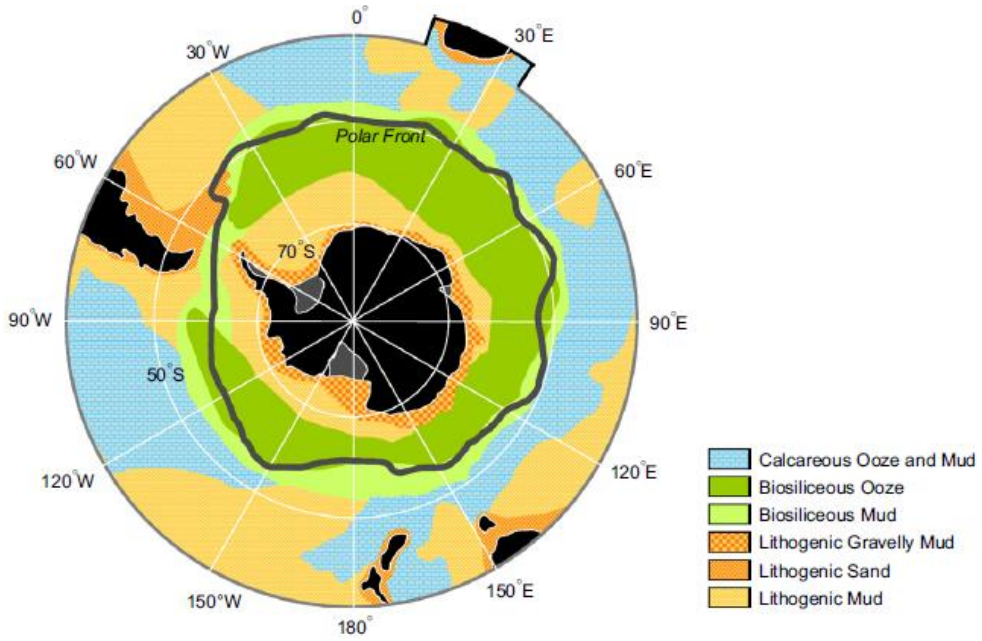

Fig. 2. Lithology of modern sediments in the Southern Ocean (from Diekmann, 2007).

1.2.2. Diatoms: a tool to decipher Southern Ocean Paleoclimate

Diatoms are unicellular algae having their cell enclosed in a amorphous silica box [Si(H2O)n] called frustules, which comprises of two intricate valves (the larger one is the epivalve and the smaller one is the hypovalve). They are placed under the class Bacillariophyceae, in which two orders were defined based on the shape of the frustule: Centrales (round diatoms) and Pennales (elongated diatoms). The Order Centrales is divided in three suborders based on the shape of the cells, the polarity and the arrangement of the processes. The Order Pennales is divided in

two suborders, one having diatoms with a raphe (an elongated slit or pair of slits within the valve wall), the other one including diatoms without a raphe. Diatom size varies from 2 μm to 1-2 mm. Diatoms generally reproduce through vegetative division at a rate of 0.1-8 times per day (Smetacek, 1985). Vegetative reproduction leads to the formation of 2 new hypovalves from the parent diatom frustule, which progressively results in the reduced average size of the diatom. At a particular threshold, physiologically dictated, diatoms undergo a sexual reproduction through gamete fusion and the formation of an auxospore that reintroduces a full-sized vegetative cell (Round, 1972). Few species have additional specific stage, the resting spore, which is formed under adverse conditions (depleted nutrient levels, low light levels, etc.) and allows the diatom survive until favourable conditions reappear (Horner, 1984).

In polar oceans, around 1-10% of the diatoms thriving in the surface waters are preserved in the ocean sediment (Ragueneau et al. 2000). This percentage escalates in shallow coastal areas relative to abyssal open ocean zones. The key processes determining the diatom flux to the sea-floor are the abiotic factors such as lateral transport and dissolution in the water column and at the water-sediment interface and biotic factors such as sedimentation type (single particles vs aggregates or fecal pellets, mass sedimentation events). These processes no only aids to the preservation of heavily silicified diatoms but also change the geochemical signals archived in the diatoms. Nevertheless, it has been depicted that the residual sedimentary assemblages still correspond to the surface conditions in different oceanic regimes like the North Pacific (Sancetta 1992) and Southern Ocean (Armand et al., 2005; Crosta et al., 2005a; Romero et al., 2005).

In high latitude oceans, diatom distribution (as phytoplankton) has a strong zonation in surface waters (Hasle, 1969; Simonsen, 1974; Semina, 2003) which is in turn reflected in the diatom distribution in surface sediments (Defelice and Wise, 1981; Sancetta, 1992; Zielinski and Gersonde, 1997). Hence it is possible to straightaway relate the diatom assemblages in surface sediments and modern parameters such as, sea-surface temperatures (SST) and sea ice duration/concentration. This hypothesis of linking diatom assemblages in fossil down-core sediments and surface parameters is known as actualism. A certain diatom assemblage is produced, and preserved, under specific modern conditions.

If the same assemblage is present in the down-core, then past oceanographic and climatic conditions may resemble the present-day condition. In Southern Ocean diatom becomes one of the most promising proxies considering the fact that the calcareous microfossils are sparse for paleoceanographic reconstruction in high latitude oceans. Hence diatoms are a robust and useful proxy to infer paleoceanographic and paleoclimatic changes in such regions.

1.3. Objectives

The basic aim of this study is to use diatom bound climate signals to offer further knowledge in understanding climate variability in the late Quaternary in the vital regions of Indian sector of Southern Ocean. This thesis aims in:

1. Studying the diatom absolute abundance as a paleoclimate indicator;
2. Investigating the morphometric variability in diatoms and its implications for Southern Ocean paleoceanography;
3. Late Quaternary reconstruction of the climate history of the Indian sector of Southern Ocean.

Chapter 2

Materials and methods

2.1. Study Area: The Indian sector of the Southern Ocean

The present study focuses on two sediment cores located in the western Indian sector of Southern Ocean (Fig.1). The Antarctic Circumpolar Current (ACC), driven by strong southern westerly winds (Rintoul, et al., 2001), flows eastward around the Antarctic continent between ~45°S and 65°S. The ACC consists of multiple hydrological fronts where the flow is strongest (Sokolov and Rintoul, 2009 a, b). In the western Indian sector of SO the presence of several subantarctic islands, such as Prince Edward Island, Marion Island and Crozet Islands, and shallow rises, such as Del Caño Rise Conrad Rise, significantly affect the ACC flow and associated fronts (Fig. 1) (Pollard and Read, 2001; Pollard et al., 2007). More specifically, the SAF-associated jets flow anticyclonically round the Del Caño Rise west of the Crozet Plateau, then northward and occasionally north-westward into the Crozet basin, before turning back eastward (Fig. 1). This S-bend in the SAF is a permanent feature controlled by bathymetry (Fig 1) (Pollard and Read, 2001; Pollard et al., 2007). Similarly, the APF is divided in two branches, one located north and the other one located south of the Conrad Rise (Sokolov & Rintoul 2009b). Extremely weak circulation prevails to the north of the Crozet Island, such weak circulation promotes the build-up of dissolved iron from the land or sediments of the Crozet Islands during the winter in the Polar Frontal Zone between Crozet and the SAF, which results in an annual bloom in this area (Pollard et al., 2007). Overall, the oceanographic fronts and winter sea ice extent allow the subdivision of the SO into a series of latitudinal zones such as sea-ice zone (SIZ), permanent open ocean zone (POOZ), polar frontal zone (PFZ) and sub-Antarctic zone (SAZ) (Treguer and Jacques, 1992; Orsi et al., 1995; Belkin and Gordon, 1996; Pollard et al., 2002).

Western Indian sector of Southern Ocean is characterized by the prevalence of sub-Antarctic islands such as Prince Edward Island, Marion Island and Crozet Islands (Fig. 1). The Marion Island (46°55′S, 37°45′E) and Prince Edward Island (46°39′S, 37°57′E) are active volcanic sites (McDougall et al., 2001; Boelhouwers et al., 2008) with waning ice caps (Sumner et al., 2004). In the past, five volcanic and eight glacial episodes have been interpreted based on the K-Ar dating and

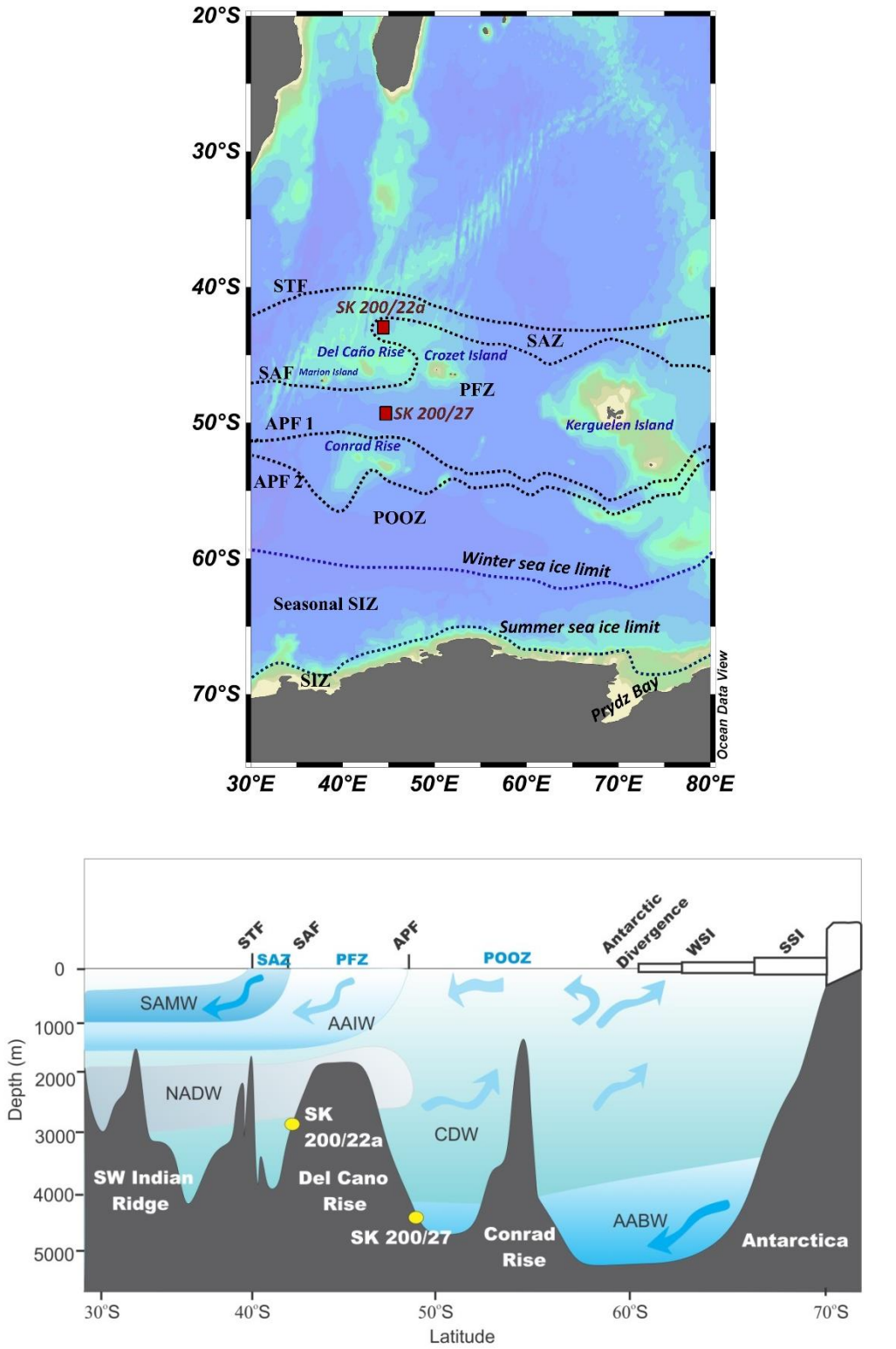

Fig.1. Study area showing the location of sediment cores SK 200/22a and SK 200/27. The positions of the Subtropical Front (STF), Sub-Antarctic Front (SAF), Polar Front (APF), and winter sea ice limit based on (Belkin and Gordon, 1996; Orsi et al. 1995; Comiso, 2003; Pollard and Read, 2001; Pollard et al., 2007: Sokolov & Rintoul 2009). Schematic view of the location of the core sites SK200/22a and SK200/27. WSI: Winter Sea Ice, SSI: Summer Sea Ice, AAIW: Antarctic Intermediate Water, NADW: North Atlantic Deep Water, AABW: Antarctic Bottom Water, CDW: Circumpolar Deep Water, SAMW: Sub-Antarctic Mode Water.

geomorphological evidences from Marion Island (McDougall et al., 2001). Such volcanic and glacial activities on Marion Island could be a significant source of terrigenous material to the adjacent waters (Thamban et al., 2005; Manoj et al., 2012) thereby influencing the biological productivity in the present as well as in the past. The Crozet Island (46°25′S, 51°38′E) comprises of five important oceanic islands placed to the east of Marion Island. They are volcanic and presently free of ice, nevertheless there are strong evidences of glacial erosion (Lebouvier and Frenot, 2007; Quilty, 2007) indicating the presence of Quaternary glaciers possibly predating the LGM (Camps et al., 2001; Giret et al., 2003; Hall, 2009).

Certain water masses such as Antarctic Bottom Water (AABW), Circumpolar Deep Water (CDW) and the Antarctic Intermediate Water (AAIW) play a vital role in the Indian sector of Southern Ocean (Fig.1). In the North Atlantic, surface waters cools and sinks at deeper depths through convection and spreads as North Atlantic Deep Waters (NADW) across the Indian and Pacific Oceans via the Southern Ocean through thermohaline circulation. At the present study site, the NADW mixes with other water masses through upwelling and gets transformed into fresh lower CDW (Callahan, 1972; Park et al., 1993).

Substantial amount of NADW is transformed into CDW in SAF region indicating that SAF is the source of CDW (You, 2000). NADW merges with CDW in South Atlantic, characterised by salinity maxima between 2000 and 3500 m, and then flows into the southwest Indian Ocean, south of Africa between 35 S° to 40°S (Charles and Fairbanks, 1992; You, 2000). NADW is restricted to the Southwest Indian Ocean by ridges in the east and north, and which makes CDW as the only key source for Indian deep circulation and ventilation in the north (You, 1999). The sediment transport and advection are largely influenced by the CDW and AABW within the ACC (Dezileau et al. 2000).

2.2. Sediment cores details

Sediment cores SK200/22a and SK200/27 were retrieved on board ORV Sagar Kanya (SK) in the Indian sector of the Southern Ocean using a piston corer (Thamban, 2005). Site SK 200/22a is located at the modern SAF north of Del Caño Rise, while core site SK 200/27 is located north of the modern northern branch of

the APF and is located in between Del Caño Rise to the north and Conrad Rise to the South.

Core	Latitude	Longitude	Water depth (m)	Core length (cm)	Coring device	Cruise
SK200/2a	43° 41′.50	45° 04′.30	2720	754	Piston Corer	ORV Sagar Kanya 200 (2004)
SK200/27	49°00′.34	45° 13′.11	4377	489		

Table.1. Sediment cores details.

Sediment core SK200/22a comprised of alternating layers of calcareous white to grey sandy silt/clay up to the depth of 115 cm, followed by a dark greyish band consisting of silty clay between 130-148 cm, and light-grey clays below this band. While, the sediment core SK200/27 comprised of alternate layers of greyish orange clayey sediments and light olive grey sandy sediments (Manoj, 2014). Layers of carbonaceous and siliceous sediments were also seen. But the core is mainly dominated by diatom oozes (Manoj et al., 2015). The studied interval of both the cores focuses on the past ca. 95 ka BP (95,000 years before present) and 75 ka BP before present (chronology described in next section), which documents the glacial-interglacial variability in Antarctic winter sea-ice and Southern Ocean frontal system, late Quaternary changes in diatom productivity and morphometric variability of *Fragilariopsis kerguelensis* and *Thalassiosira lentiginosa*.

2.3. Chronology

The age models for the sediment cores SK 200/22a and SK 200/27 are based on Accelerator Mass Spectrometry (AMS) radiocarbon (^{14}C) dates measured on the planktonic foraminifers, supported by correlation of the stable isotope and

geochemical profiles of the cores with the stacked oceanic and ice core records from Southern Hemisphere (Manoj, 2014; Manoj and Thamban, 2015). In SK200/27, owing to the absence of calcitic foraminiferal tests below 75 -80 cm, additional chronology was obtained using AMS ^{14}C dating of the total organic carbon in the sediments (Table 2). The radiocarbon ages were calibrated to calendar ages, utilizing the Calib 6 (Stuiver et al., 2005) with a reservoir age correction of 850 years (Bard, 1988; Berkman and Forman, 1996; Dutta, 2008) and all dates are cited as calendar years BP in the text. Despite the spatial and temporal differences in the reservoir ages within the different sectors and frontal regimes of the Southern Ocean, it is well within the chronological uncertainties of the cores. As per the studies done by Manoj (2014), chronology beyond the limits of conventional radiocarbon dating was accomplished by correlating the planktonic and benthic $\delta^{18}O$ data with the established Antarctic ice core records (Byrd and EDML) (Blunier and Brook, 2001; EPICA Community Members, 2006), and LR04 $\delta^{18}O$ Stack (Lisiecki and Raymo, 2005) as well as records from the Drake Passage in the Southern Ocean (Bae et al., 2003). The final age model depends on a linear interpolation between the control points, presuming that the signals recorded in the Southern Ocean sediment cores and Antarctic ice cores are in close association with the climate variability in the rest of the Southern Hemisphere. The 7.54 m of the sediment core SK200/22a spanning 95 ka BP consists of the Marine Isotope Stage (MIS) 1, 2, 3, 4 and later part of MIS 5 (Manoj, 2014). The sedimentation rate for different intervals of the core ranges from 0.93 cm/ka to 6.85 cm/ka and is highest for glacial sediments (Manoj, 2014). The other core SK200/27 having length 4.89 m represents 75 ka BP (Table.2).

Cores	Depth interval in the core (cm)	Radiocarbon age (years)	Error (±)	Calibrated age (years)	Remarks
	8-10	2635	36	2764± 16	
	40-42	5590	35	6368 ± 37	
	76-78	8822	46	9929 ± 151	

SK 200/22a	128-130	10943	70	12885 ± 98	Planktic foraminifera
	144-146	13881	68	17124 ± 200	
	180-182	17186	88	20636 ± 295	
	196-198	32300	160	36635 ± 571	
	222-224	34000	250	39580 ± 948	
	248-250	35090	630	40051 ± 953	
	310-312	37200	250	41956 ± 324	
SK 200/27	08-10	2632	75	2713 ± 115	
	48-50	10164	54	11817 ± 164	
	68-70	11017	55	12924 ± 104	
	96-98	16050	200	19212 ± 285	Organic carbon
	144-146	20200	310	24117 ± 438	
	232-234	23200	550	27879 ± 820	

Table 2. AMS ^{14}C ages determined from core SK 200/22a and SK 200/27, calibrated calendar ages after Stuiver et al. (2005).
*** Samples measured at (a) NSF-AMS Facility of the Arizona University and (b) NOSAMS facility at Woods Hole, USA.**

2.4. Sediment processing and diatom analysis

Protocol adopted for sediment processing and slide preparations for diatom counts were based on the techniques described by Batterby (1986) and Gersonde and Zielinski (2000). Dried sediment sample of 0.1-0.5 g of weight were treated with ca. 15-20 ml of hydrogen peroxide (H_2O_2, 35%) in a 500 ml beaker and heated to fasten the chemical reaction and getting rid of the peroxide through evaporation. Later when the samples cooled to room temperature few drops of concentrated hydrochloric acid (HCl) is added. Upon completion of the reaction, distilled H_2O was added to the samples up to 500 ml. The water was decanted after a settling of 8-10 hrs. This decantation process was done 5-6 times to get rid of all the acid and clay part. The residue was then shifted to a 50 ml bottle and diluted to 50 ml for archiving followed by the addition 2 or 3 drops of neutralized formaldehyde for preservation. For permanent slide preparations coverslips were placed in a petri-

dishes filled with purified water. A specific aliquot (based on the concentration of diatom valves) was randomly suspended in the petri-dish from the centre of the homogenized suspension from the 50 ml bottle. After 1-2 hr of settling duration the water was drained out of the petri-dish and coverslips were allowed to dry. Coverslips were then subjected to permanent mounting using Naphrax as a mountant.

Diatom counts were done referring to Schrader and Gersonde (1978). Numerous traverses across each cover slip were examined, around 350-900 valves were counted, depending on the diatom abundances, in each sample at a magnification of ×1000 utilizing an inverted light microscope (Nikon Eclipse *Ti*-U). Taxonomy of diatoms followed Hasle and Syvertsen (1997), Scott and Thomas (2005), Round et al. (1990), and Cefarelli et al. (2010).

As per to Schrader and Gersonde (1978) and Zielinski (1993) the below listed diatom frustule fragments were counted as single valve (Fig. 2):

A. Centric diatoms such as *Actinocyclus, Thalassiosira* with or without pseudonodulus when greater than half of the valve was present;
B. *Chaetoceros* sp., when greater than half of the frustule was present;
C. Centric diatoms such as *Eucampia Antarctica* having horns, when greater than half of the frustule with horn were counted as one;
D. Araphid diatoms such as *Thalassionema, Thalassiothrix* having two apices of the valve were considered as one valve;
E. Diatoms genus such as *Fragilariopsis* having canal raphe greater than half of the valve was considered as single valve, or when only central portion is present without the apices were counted as one valve;
F. Mono- or biraphid diatoms such as *Navicula,* section having central nodule or greater than half of the frustule were considered as single valve; G. *Rhizosolenia* sp., valve having process and apices were considered as one valve.

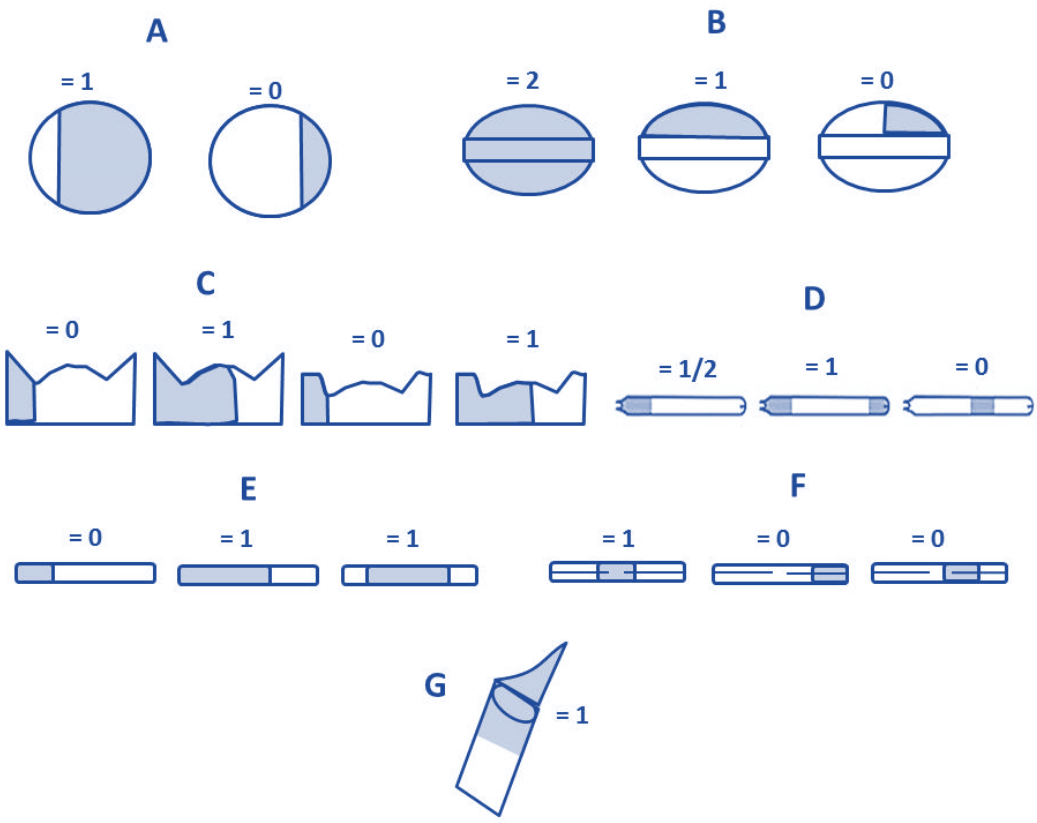

Fig.2. Schematic diagram of the norms in counting diatom valves (after Xiao, 2011; Zielinski, 1993).

2.5. Diatom morphometry

Two species of diatom, *F. kerguelensis* (pennate) and *T. lentiginosa* (centric) were chosen for morphometric studies owing to their high relative abundances in the Southern Ocean and their significance in carbon and silica cycling (Cortese & Gersonde 2007, Abelmann et al. 2015; Shukla et al., 2013, 2016). Manual measurements of the length of apical axis of *F. kerguelensis* and radius of *T. lentiginosa* were done using Nickon eclipse Ti-U inverted microscope along with the nuclear inelastic scattering (NIS) element imaging software on a computer. Sizes of these diatoms were measured for every 2 cm depth interval up to 200 cm depth and there on every 5 cm interval up to 754 cm depth in the sediment core SK 200/22a, while for the sediment core SK 200/27 measurements were done for every 2 cm interval upto 489 cm. Measurements were performed on nearly 80 specimens each of *F. kerguelensis* and *T. lentiginosa* (depending on the abundance of these species) on the same diatom slides used for diatom census counts.

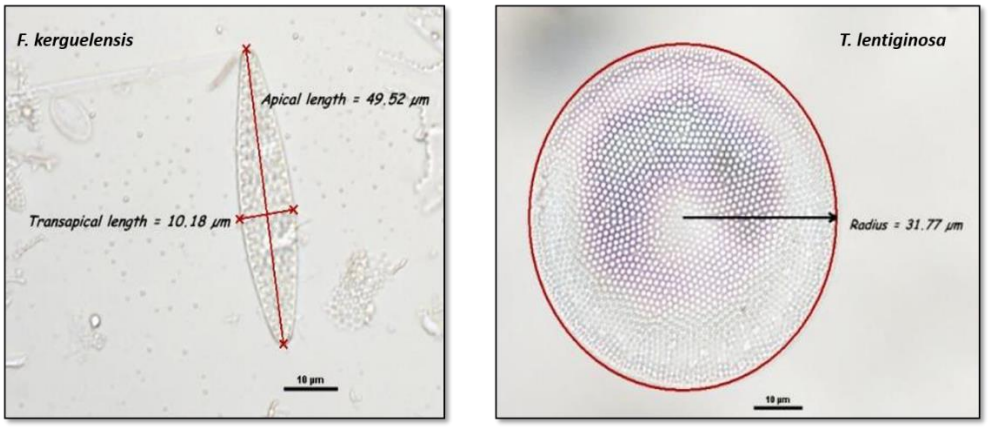

Fig.3. Apical and trans-apical length of *F. kerguelensis* and radius of *T. lentiginosa.*

2.6. Seas surface temperature and sea ice estimation

Summer SST (January-February-March) and sea-ice duration reconstruction were estimated by applying the Modern Analog Technique (MAT) to fossil diatom assemblages. The modern database is composed of 249 surface sediment samples (modern analogs) for which locations modern summer SST were interpolated on a 0.25°*0.25° grid from the World Ocean Atlas 2013 (Locarnini et al., 2013) using Ocean Data View and monthly sea-ice concentration data were interpolated on a 1°*1° grid from the numerical atlas of Schweitzer (1995) covering the 1978-1994 period. Annual sea-ice duration is represented as the number of months per year of sea-ice cover over each core-top location. Yearly sea-ice duration is the sum of monthly sea ice values whereby 0 month per year is attributed to ice-free areas (0-15% sea ice concentration), 0.5 month per year is attributed to unconsolidated sea ice (15-40% sea ice concentration) and 1 month per year is attributed to consolidated ice (40-100 % sea ice concentration) (Armand et al., 2005).

The MAT is based on the principle that similar species assemblages derived from similar environments (Prell, 1985). The MAT used here was implemented from the "bioindic" package (Guiot and de Vernal, 2011) built on the R-platform (http://cran.r-project.org/). We used here the relative abundances of 32 diatom species and the chord distance to select the five most similar modern analogs. The threshold above which modern analogs are supposed to be too dissimilar to the fossil assemblage is fixed at the first quartile of random distances on the validation/modern dataset. Quantitative estimates of summer SST and sea-ice

duration represent a distance-weighted mean of the climate values associated with the selected modern analogs (Guiot et al., 1993). This method yields a R2 of 0.96 and a root mean square error of 1.04°C for summer SST and a R2of 0.96 and a root mean square error of 0.85 month per year for sea-ice duration.

Chapter 3

Annotated index of key diatom species

3.1. Diatom Groups (Light Microscope and Scanning electron microscope studies)

The main aim of this chapter is to list out the abundant diatoms from their specific groups (SAZ, POOZ and Sea ice) as per their taxonomic description given by the respective authors. For each diatom species the page of the protologue and the figure is cited. Diatoms from Southern Ocean having similar environmental preferences (sea-ice and SSTs) were grouped on the basis of Q-mode factor analysis by Crosta et al. (1998a). Following the study of Crosta et al. (1998a), the diatom assemblages encountered here were grouped into Permanent Open Ocean Zone (POOZ) group, Sub-Antarctic Zone (SAZ) group and sea-ice group (Nair et al., 2015). The light microscope (LM) and scanning electron microscope (SEM) images of diatoms representing their respective groups are shown in the figure 1, 2 and 3.

3.1.1. Sub-Antarctic Zone diatoms (Figure 1)

Hemidiscus cuneiformis Wallich Figures in: Hustedt (1930) fig. 542; Fryxell et al. (1986), fig. XXVI.

Description: Cells are wedge shaped. Valve are flat, almost semi-circular with dorsal margin strongly convex and ventral margin weakly convex, often with a median inflation on the ventral side. Apical axis ranges from 40-174 µm and transapical axis ranges from 30-90 µm. Towards the valve centre the areolae are arranged in irregular radial fascicles, but in short parallel lines, with 6-12 areolae in 10 µm. Whereas towards the margin the areolae are irregular or tangential with 10-18 areolae in 10 µm. Poles are characterised with small inconspicuous processes, whereas central hyaline area (Fig 1A, B) and rosette is absent. Ventral margin of the valve is punctuated with small spinules and a small partially occluded pseudonodulus midway along the margin. Labiate processes 1-2 numbers in 10 µm along the ventral margin only, with 1 on either side of the pseudonodulus. Girdle simple, lacking intercalary bands. Chloroplast numerous, small, spherical. *Hemidiscus cuneiformis* is a typically a warm-water diatom (Hasle and Syvertsen, 1996; Semina, 2003). It occurs in low numbers, and is a sporadic component of diatom assemblages found in the Arabian Sea and Indian Ocean (Simonsen, 1974), and sediment traps from the Atlantic Ocean south of the equator (Romero et al.,

2005). Highest abundance of this species is reported to be ~7% in the surface sediments during the Austral summer at SST of >15°C, yet occasionally it occurs between the SST range of 7-20°C in South Atlantic (Zielinski and Gersonde, 1997).

Azpeitia tabularis var. *tabularis* (Grunow) G. Fryxell and P.A. Sims Figures in: Hustedt (1930) fig. 230a; Fryxell et al. (1986) Pl. XXX, fig. 1.
Description: Cells are solitary and discoid with pervalvar axis *c*. 7 µm. Valves are circular and flat with apical axis ranging from 16-70 µm. Areolae are slightly fasciculate and arranged in radial rows. Approximately 5-10 areolae were present in 10 µm near the centre and *c.* 16 areolae in 10 µm towards the margin. Marginal ring is marked by the presence of labiate processes (Fig 1C, D), nearly 7-12 labiate processes are present in 10 µm, laterally expanded, with a reduced neck. Labiate process solitary, large, located on the edge of the central annulus. Pseudonodulus is absent. *Azpeitia tabularis* is actually a tropical/subtropical diatom, but abundant at the north of APF in subantarctic Southern Ocean (Hasle and Syvertsen,1996; Romero et al., 2005). Maximum abundances of this species goes up to ca. 24% at warm SST's of 13°C February, 11°C August (Romero et al., 2005).

Thalassiosira oestrupii var. *oestrupii* (Ostenfeld) Hasle Figures in: Fryxell and Hasle (1980) figs 1–3, 6–7, 12–19 (variations *oestrupii* and *venrickae*).
Description: Cells are chain-forming, connected by chitinous threads from the off-central strutted process. Cells are discoid to rectangular in girdle view; pervalvar axis is 0.5-2 times larger than the valve diameter. Valves are circular with diameter ranging from 7-60 µm. Areolation is eccentric and coarse. Around 5-10 areolae are present in 10 µm at the centre, whereas 6-12 areolae are present in 10 µm near the margin. Strutted processes are trifulate and operculate, with internal extensions; 1 process in an off-centre position (Fig 1E, F) and 1 marginal ring of processes 6-8 in 10 µm. Labiate process are solitary and not marginal, internally flattened and parallel to margin. Despite cosmopolitan in its distribution and mainly tropical to temperate in its temperature likings, the species, also recorded (rarely) in the waters as far as Norwegian See and as south as the Weddell Sea (Fryxell and Hasle, 1980; Romero et al., 2005). The relative abundance of this diatom decreases north-south in Southern Ocean (Romero et al., 2005). Highest relative abundance of up to ~5% is noted mostly in the Atlantic sector of Southern Ocean north of the SAF, whereas

only minor occurrences are seen in the Indian sector (Romero et al., 2005). The relative abundance of *T. oestrupii* in surface sediment sharply increases at SST 11 °C (Romero et al., 2005).

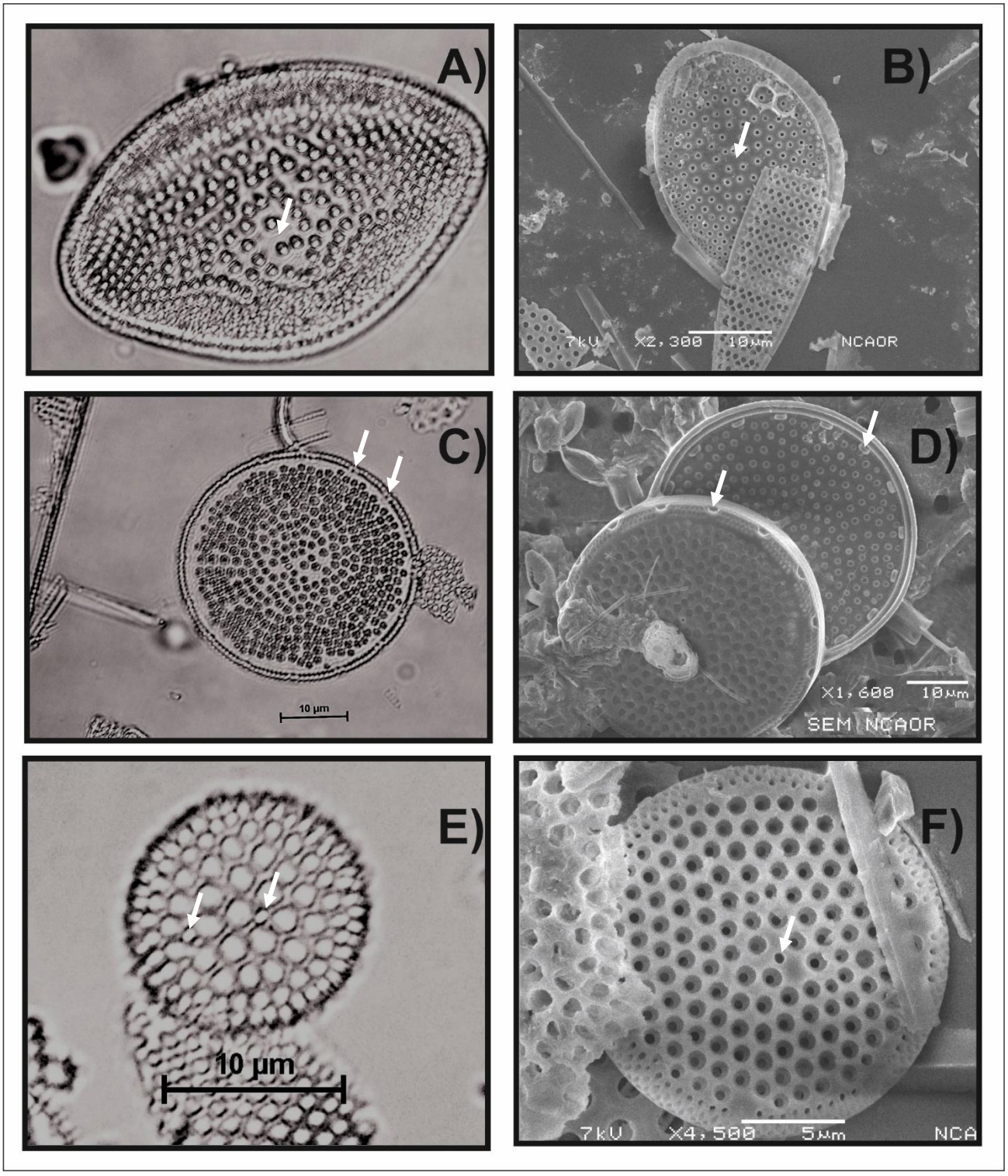

Fig. 1. SAZ diatoms: (A) *Hemidiscus cuneiformis* (central hyaline marked; LM) (B) *Hemidiscus cuneiformis* (central hyaline marked; SEM), (C) *Azpeitia tabularis* (marginal labiate processes marked; LM), (D) *Azpeitia tabularis* (marginal labiate processes marked; SEM), (E) *Thalassiosira oestrupii* (strutted process marked; LM), (F) *Thalassiosira oestrupii* (strutted process marked; SEM).

3.1.2. Permanent Open Ocean Zone diatoms (Figure 2)

Fragilariopsis kerguelensis (O'Meara) Hustedt References used: Hustedt (1958), plate 10, figures 121–127; Hasle (1965b), plate 4, figures 11–18.
Description: Cells are solitary or forming ribbon shaped colonies attached by the valve surfaces. In girdle view valve face is slightly curved towards the end and in valve view cells are elliptical. Apical axis ranges from 10-76 µm and transapical axis ranges from 5-11 µm. Transapical striae are straight and coarse with 4-7 striae in 10 µm (Fig 2A), striae near the valve poles are slightly curved. Interstrial membranes punctate, with 2 rows of alternating areolae with areolae ranging from 8-10 in 10 µm. *F. kerguelensis* is the most abundant diatom preserved in surface sediments of Southern Ocean (Crosta et al., 2005). Highest abundances of this diatom is between 70–83% which is recorded in the zone within the maximum summer sea-ice edge and the APF, where it is the main contributor of the "Diatom Ooze Belt"-defined by Burckle and Cirilli, (1987). Highest abundances are found at February SST of 1–8°C. SSTs above 8°C lead to the slow decrease in relative abundance of *F. kerguelensis*. Where *F. kerguelensis* abundance in surface sediments of Southern Ocean is less than 5% at SST 19°C (Crosta et al., 2005). The *F. kerguelensis* abundances fall sharply below 0°C and above 20°C. This diatom is also found in the surface sediment regions having ~ 8 months/year of sea-ice cover overhead, however there seems to be no preference between ice covered and ice-free regions (Crosta et al., 2005).

Thalassiosira lentiginosa (Janisch) Fryxell References for *T. lentiginosa*: Hustedt (1958), plate 4, figures 22–25; Johansen and Fryxell (1985), figures 49 and 50.
Description: Cells are solitary, discoid, narrowly rectangular in girdle view. Pervalvar axis ranges from 8-25 µm. Valves are flat, circular and 29-120 µm in diameter. Areolation usually fasciculate with 7-9 areolae in 10 µm over valve face, *c.* 15 in 10 µm at the margin, loculate, opening externally via a foramen, internally via cribrum. Strutted processes scattered evenly over valve face, resembling small areolae, 3-4 in 10 µm, lacking internal and external tubes. Labiate process solitary, marginal internal opening slit- like (Fig 2D), with radial orientation. Chloroplast small and numerous. The distribution of *T. lentiginosa* in Southern Ocean is similar to that of *F. kerguelensis* (Crosta et al., 2005). Highest abundances of *T. lentiginosa*

are reported from the maximum winter sea-ice edge to the SAF (Crosta et al., 2005). Their occurrences further decrease towards SAZ and STF. Maximum abundance of ~30% is observed in the SST range between 1-8°C and their abundance decreases at SST below 1°C (Crosta et al., 2005).

Thalassiosira gracilis group (Karsten) Hustedt References for *T. gracilis* var. *gracilis*: Hustedt (1958), plate 3, figures 4–7; Fryxell and Hasle (1979), figures 12–22.

Description: Cells are solitary or chain-forming, discoid and heavily silicified with a thin chitinous strand from the central strutted process. Pervalvar axis is 3.5-9.5 µm. Valves flat, circular and 5-28 µm in diameter. Areolation coarse with areolae ranging from 8-12 in 10 µm in the centre, and 16-20 in 10 µm towards the margin. Presence of loculate, opening externally via a simple foramen and internally via a finely pored velum. Strutted process is solitary in the valve centre or off-centre (Fig 2E, F) with a single ring of process at the margin, 3-4 processes in 10 µm; processes with internal extensions are operculate. Labiate process solitary, located *c.* one-third of the distance from margin to valve centre. Abundances of the *T. gracilis group* increases towards the region of maximum winter sea-ice extent and the Antarctic coast (Crosta et al., 2005). Whereas, to the north of APF, this group is present in trace amounts. Highest abundances of *T. gracilis group* is associated with February SST between 1 and 2°C (Crosta et al., 2005). This group has increasing occurrences with the increasing sea ice duration to a maximum of 8.5 months per year (Crosta et al., 2005).

Thalassiosira oliverana (O'Meara) Makarova et Nikolaev References for *T. oliverana*: Fenner et al. (1976), plate 14, figures 1–5; Akiba (1982), figures 1–5.

Description: Cells are discoid and valves are circular with a diameter of 23-60 µm. Areolation radial to irregular, fine to coarse; areolae 7-8 in 10 µm in the centre, 9-14 in 10 µm near the margin; marginal band is broad and distinctive with fine areolation. Strutted processes in 1 marginal ring within marginal band, 3 strutted processes in 10 µm (Fig 2H). Labiate process solitary, large, near the margin. The species *T. oliverana* has, what seems like, a ubiquitous distribution in sediments of the Southern Ocean. At the Antarctic coast, their abundances decrease and seldomly rare (Crosta et al., 2005). This species is highly abundant between the

maximum winter sea-ice edge and the APF. *T. oliverana* maximum abundance of 4-5% lies between 2 and 4°C February SST (Crosta et al., 2005). It generally shows a decreasing trend from open ocean to prolonged sea ice cover regions (Crosta et al., 2005).

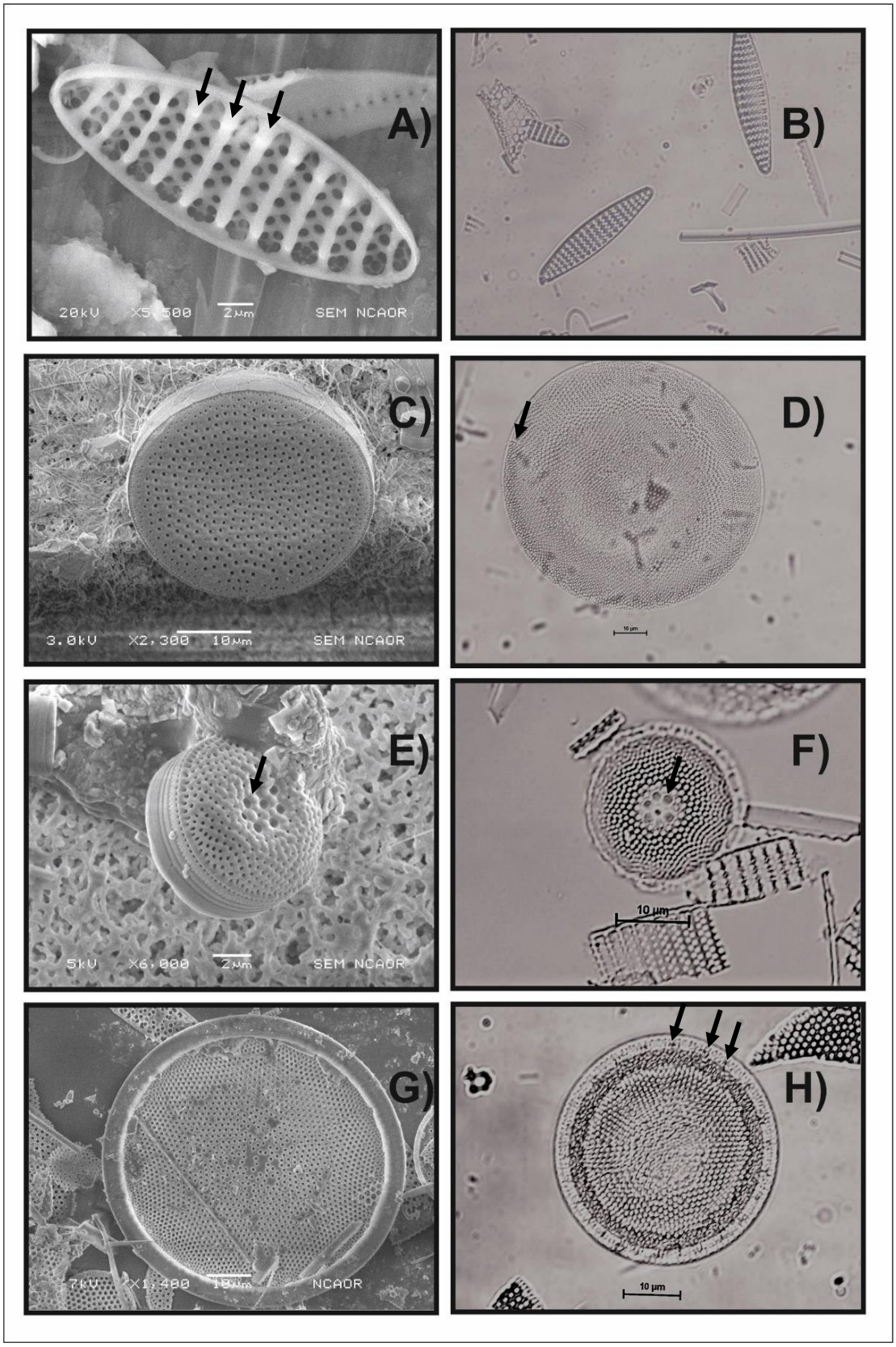

Fig. 2. POOZ diatoms: (A) *Fragilariopsis kerguelensis* (trans-apical striae marked; SEM), (B) *Fragilariopsis kerguelensis* (LM), (C) *Thalassiosira lentiginosa* (SEM), (D) *Thalassiosira lentiginosa* (labiate process marked; LM), (E) *Thalassiosira gracilis* (strutted processes marked; SEM), (F) *Thalassiosira gracilis* (strutted processes marked; LM), (G) *Thalassiosira oliverana* (SEM), (H) *Thalassiosira oliverana* (strutted process marked; LM).

3.1.3. Sea ice related diatoms (Figure 3)

Fragilariopsis curta (Van Heurck) Hustedt Figures in: Hustedt (1958), Pl. 11, Figs. 140–144;
Hasle (1965), Pl. 12, Figs. 2–5, Pl. 13, Figs. 1–6.
Cells are solitary or chain forming attached by the valve surfaces, linear in valve view, with rouned poles, one broader than the other. Apical axis 10-42 µm, transapical axis 3.5 -6 µm. Transapical striae 9-12 in 10 µm, straight, but striae near valve poles are curved (3A, B). Interstrial membranes perforated by 1-2 or 2-3 rows of areolae, *c*. 30 in 10 µm. Fibulae present in slightly lower numbers than striae, comparatively broad and irregularly placed. Pseudonodulus absent. Terminal nodules not confirmed (Hasle, 1965b). The Maximum geographical range of *F. curta* is limited southwards from maximum winter sea ice edge (Armand et al., 2005). *F. curta* has maximum abundance in sediments near the Antarctic cost (Zielinski and Gersonde, 1997; Armand et al., 2005). The highest abundances (60-70%) are associated with Southern Ocean regions having 9–11 months/year sea ice cover (Armand et al., 2005). *F. curta* prefers SST range of -1.3 to 2.5°C, having maximum abundance of ~70% falling within SST of 0.5-1 °C (Armand et al., 2005).

Actinocyclus actinochilus (Ehrenberg) Simonsen Figures in: Villareal and Fryxell (1983), Figs. 21– 24; Zielinski (1993), Pl. 1, Figs. 1 and 3.
Cells are solitary and cylindrical to discoid. Valves are flat with rounded edges with diameter ranging from 20-112 µm. Areolae are arranged in isolated radial rows that are sometimes curved or incomplete (Fig 3C, D). Areolation is variable with 5-11 areolae in 10 µm, loculate, with a foramen on the inside, bordered by a thickened rim. Marginal labiate processes 1 in 10 µm, 9-15 µm apart, laterally expanded. Pseudonodulus sometimes present near junction of flat part of valve face and mantle, not perforate. Striae on valve mantle 13-21 in 10 µm. Chloroplasts numerous, discoid. In the Southern Ocean surface sediments, *Actinocyclus actinochilus* has highest abundance of 2.9% associated with February SST between 0 and 1 °C (Armand et al., 2005). The abundance of this species increases to >2% when there is 8-9 months/year sea ice cover in Southern Ocean (Armand et al.,

2005). Their abundance normally decreases from coastal Antarctica to maximum winter sea ice edge (Armand et al., 2005).

Fragilariopsis ritscheri Hustedt Figures in: Hustedt (1958), Pl. 11 Figs. 133–136; Hasle (1965), Pl. 1, Fig. 20; Pl. 4, Figs. 1–10; Pl. 15, Figs. 12–13; Pl. 17, Fig. 8.
Description: Cells are solitary or in chains; small cells linear to elliptical in valve view, large cells linear to lanceolate and broader at one pole. Apical axis ranges from 22-60 µm and transapical axis ranges from 8-9 µm. Transapical striae straight in the middle of the cell, curved near the valve poles; striae adjacent to broad pole more oblique than at narrow pole 6-8 in 10 µm (Fig 3E, F). Fibulae curved, present in the same numbers as striae. Pseudonodulus is absent. Canal raphe present, but not always obvious. Highest abundance of *F. ritscheri* is observed with SSTs ranging from 0-3°C and sea ice duration varying from 2-10.5 months/year (Armand et al., 2005). The highest recorded abundance of *F. ritscheri* was 3.28% in the Ross Sea (Cunningham and Leventer, 1998), whereas Zielinski and Gersonde, (1997) reported a maximum of 2.6% in the South Atlantic sector (Armand et al., 2005).

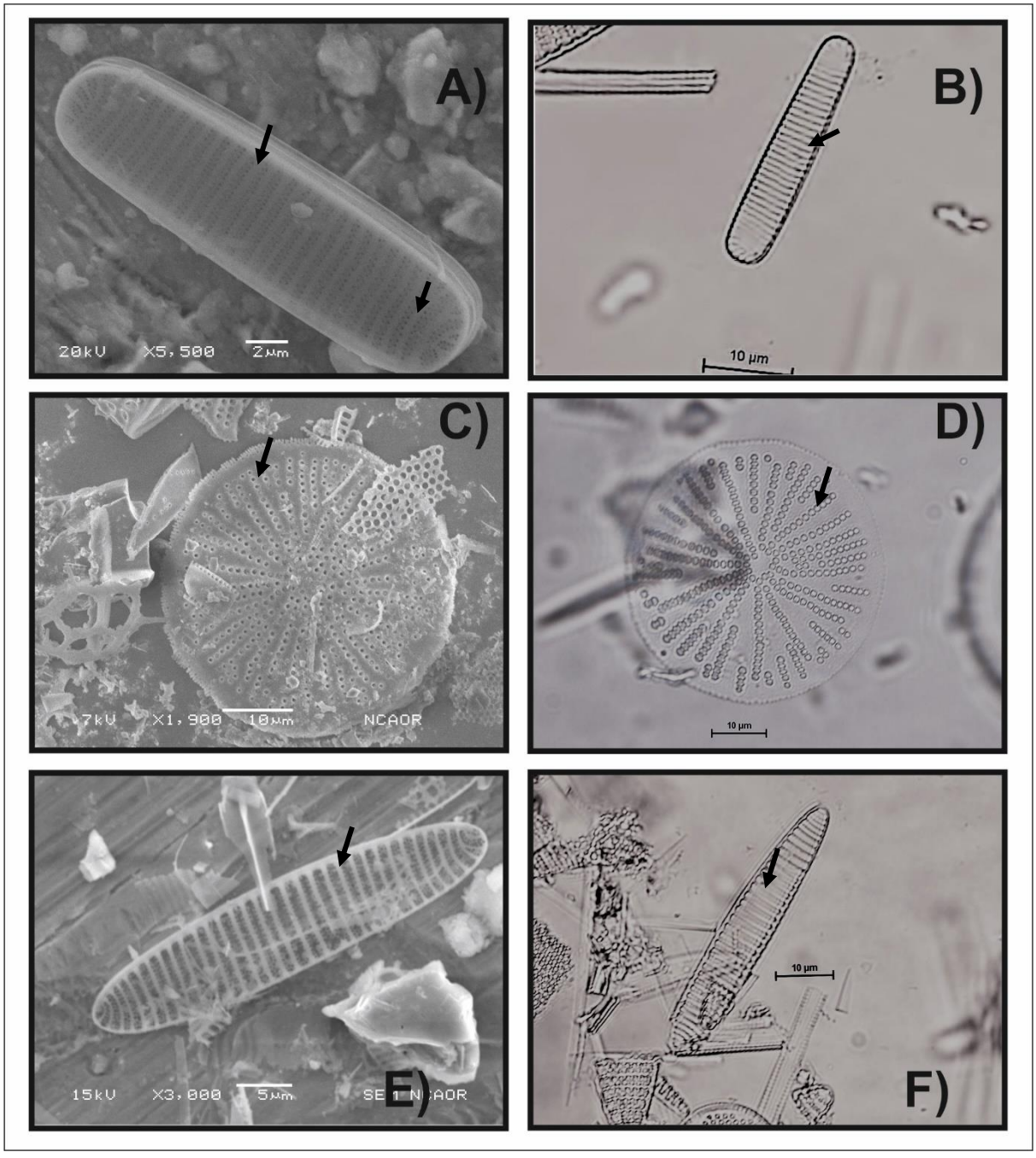

Fig.3. SIZ diatoms: (A) *Fragilariopsis curta* (trans-apical striae marked; SEM), (B) *Fragilariopsis curta* (trans-apical striae marked; LM), (C) *Actinocyclus actinochilus* (areolae marked; SEM), (D) *Actinocyclus actinochilus* (areolae marked; LM), (E) *Fragilariopsis ritscheri* (trans-apical striae marked; SEM), (F) *Fragilariopsis ritscheri* (trans-apical striae marked; LM).

Chapter 4

Variability in diatom abundance and valve size during the glacial-interglacial periods and their implications for Southern Ocean paleoceanography

4.1. Background

The Southern Ocean (SO) circulation is a vital component of the global climate system because of its impacts on the global meridional overturning circulation (MOC), heat uptake and global carbon budget (Toggweiler and Samuels, 1993; Sabine et al., 2004; Stouffer et al., 2006; Le Quéré et al., 2007). The Antarctic Circumpolar Current (ACC), flowing between ~35°S and ~65°S, is the most vital junction in the global ocean circulation system as it closes the MOC and redistributes waters from the Atlantic Ocean to the other oceans. The ACC also plays a vital part in the Antarctic ice system by curtailing the flux of surface subtropical heat into the SO, thus thermally isolating the Antarctic continent. The ACC embeds several oceanographic frontal systems, the Antarctic polar front (PF), the sub-Antarctic front (SAF), and the subtropical front (STF) that separate the SO into the Subantarctic Zone (SAZ), the Polar Front Zone (PFZ), and the Antarctic Zone (AZ) (Treguer and Jacques, 1992; Orsi et al., 1995; Belkin and Gordon, 1996; Pollard et al., 2002). The PFZ and AZ are nutrient-rich and support high siliceous productivity, especially in the vicinity of the APF and coastal Antarctica, while nutrients decrease in the SAZ and Subtropical Zone where productivity is dominated by calcareous organisms (Ragueneau et al., 2000).

Climate model studies have shown a clear picture of how the ACC as an entity might be expected to respond to a poleward shift and intensification of westerlies (Downes et al., 2011). Northward migrations of the ACC and associated fronts, along with expansion of the winter sea ice cover, have been suggested to occur during glacial periods of the Quaternary (Gersonde and Zielinski, 2000; Crosta et al., 2004). Focusing on the Last Glacial Maximum (LGM), a migration of 5-10° of latitude was documented for Antarctic Polar Front (APF) and Sub-Antarctic Front (SAF) and an expansion of the winter sea-ice cover by 7-10□ of latitude in the Indian sector of the SO (Gersonde et al., 2005). Northward migration of the hydrological fronts and expansion of the sea ice system during the LGM were attributed to a northward displacement of the ACC, forced by similar northward migration of the Southern Hemisphere Westerlies winds (SWW) and lowering of both atmospheric and oceanic temperatures (Gersonde et al., 2005; Toggweiller et al., 2006; Ferry et al., 2015).

Investigating the diatom content of two cores across the main hydrological fronts of the SO Indian sector we here reconstruct SST and sea ice duration along with diatom productivity and infer the meridional displacements of the ACC over the past 95,000 years (ka).

4.2. Materials and methods

The details of methodology and study area have been mentioned in the chapter 2.

4.3. Results

4.3.1. Glacial-interglacial changes in sedimentary records of SK 200/22a

Diatoms from the POOZ group dominate the assemblages in SAF (mean of 82.7%) core site (Fig 1b). The contribution of POOZ diatoms was lower during interglacial periods, with relative abundance as low as ~68% during MIS 5 and ~70 % in MIS 1. Similarly, the SIZ diatom group displayed an obvious glacial-interglacial pattern with highest relative abundances during glacial periods, reaching ~5% of the total diatom assemblages during MIS 4 and 3-4% between late MIS 3 and MIS 2, and lowest relative abundances during interglacial periods, been almost absent during MIS 5 and MIS 1 (Fig 1c). The SAZ group diatoms accounted for 15-23% and 10-15% during MIS 1 and MIS 5, respectively (Fig 1a). Relative abundances were lower (~5%) during the MIS 4-2 period. Notably, maximum relative abundances of the SAZ group were encountered during the MIS 2-1 transition.

Summer SST reconstructed for the SAF core site (SK 200/22a) vary between 2°C and 5°C (Fig 1d). Summer SST were around 4°C during the late MIS 5, MIS 3 and MIS 1. The warmest SST, around ~5°C, occurred during the last deglaciation (~14 ka BP) and mid-MIS 1 (~5 ka BP). SSTs were around 3°C during MIS 4 and MIS 2, with minima around 2°C during the LGM. Sea ice duration estimated for SAF core site reveals that sea ice occurred infrequently between 95 ky and 23 ky with values below the RMSE (Fig. 1e). However, the LGM and the 13-11 ka BP periods were characterized by values of 1-2 month/year, above the RMSE.

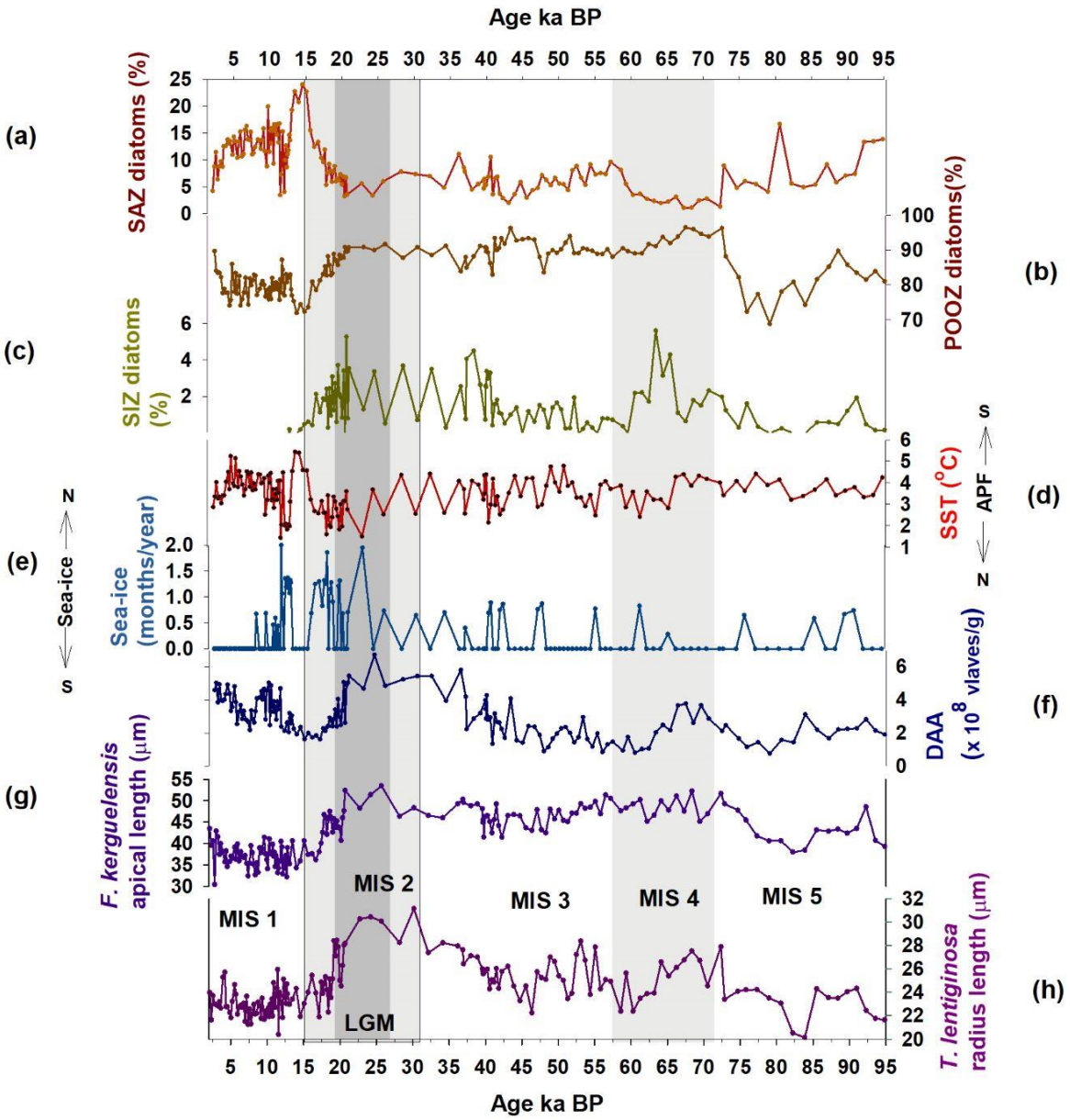

Figure 1: SK 200/22a sediment records a) relative percentage (%) of Sub-Antarctic Zone diatom group, b) permanent open ocean zone diatom group, c) Sea ice diatom group, d) summer SST, e) Sea-ice duration (months/year), f) Diatom absolute abundance (DAA), g) *F. kerguelensis* average apical length and h) *T. lentiginosa* radius. Grey periods indicate glacial periods.

The total diatom concentration varied significantly (range 0.76×10^8-6.7×10^8 valves/g of dry sediment) during the past ~95 kyr in the SAF core site (fig. 1f). Highest values (6-6.7×10^8 valves/g) were recorded during late MIS 3 to LGM, moderate values (3.7-5×10^8 valves/g) during early MIS 4, early and late MIS 1, whereas low abundances (1-1.5×10^8 valves/g) were observed during late MIS 5, MIS 4-3 transition and the last deglaciation.

In the SAF core site, the mean apical length of *F. kerguelensis* varied between ~30 µm and ~50 µm (Fig 1g). Short *F. kerguelensis* (30-40µm) were encountered during late MIS 5, late MIS 2 (last deglaciation) and MIS 1, while long *F. kerguelensis* (> 40 µm) were found during the MIS 4, MIS 3 and early-mid MIS 2 (Fig 3). Changes in *T. lentiginosa* mean radius followed a rather similar pattern with small specimens (radius of 20-24 µm) encountered during the late MIS 5 and since 18 ka BP and large specimens (mean radius of 25-30 µm) found during the MIS 4-2 period (Fig 1h & Fig 2).

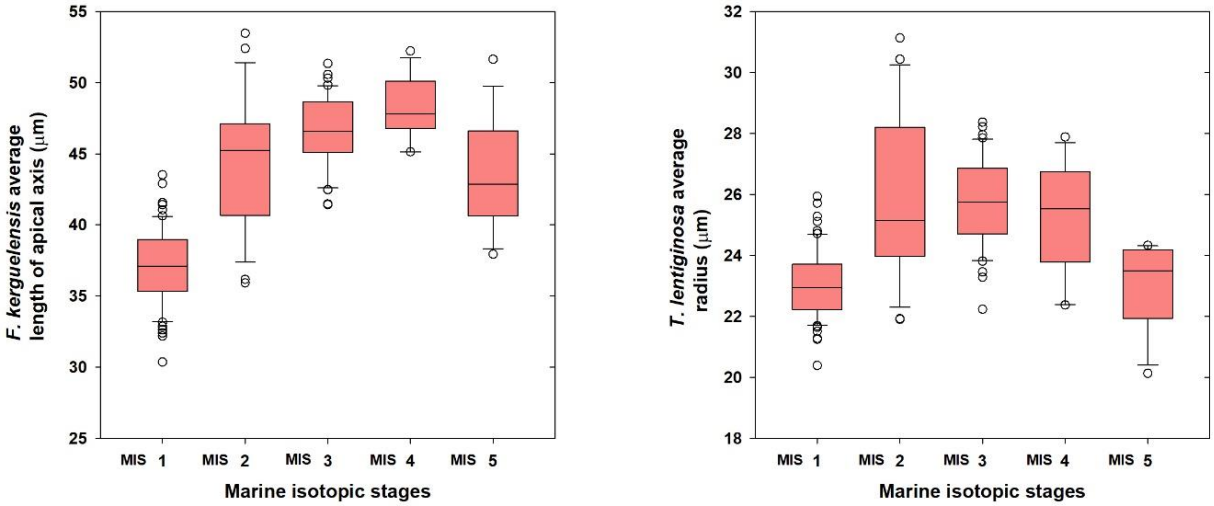

Figure 2: Box plot showing size variation of *F. kerguelensis* and *T. lentiginosa* during MIS 1-5 in SK 200/22a.

4.3.2. Glacial-interglacial changes in sedimentary records of SK 200/27

Diatoms from the POOZ group dominated the assemblages in APF (mean of 91.4%) core site (Fig 3b). The POOZ diatoms had lowest relative abundances during glacial periods as compared to MIS 1, with 75 % abundance in MIS 4, 80-85% in mid MIS 3 and ~87% during MIS 2. The SIZ diatoms showed a distinct glacial-interglacial pattern presenting highest relative abundances of ~7% during MIS 4 and MIS 2, low contribution during MIS 3 and almost absent during MIS 1 (Fig 3c). Conversely, the SAZ diatoms reached highest relative abundances during MIS 3, MIS 2-1 transition and MIS 1 (~10% and 5%, respectively) and lowest contribution during MIS 4 and MIS 2 (0-3%) (Fig 3a).

At the APF core site (SK 200/27), summer SST varied between 1°C and 4°C (Fig 3d). Warmest summer SST of ~4°C occurred during the MIS 1. Summer SST were around 2-3°C during MIS 3 and 1-3°C during MIS 4 and MIS 2. Sea ice duration is estimated at ~1 month/year during MIS 4 (Fig 3e). Sea ice retreat occurred abruptly during early MIS 3 and sea ice was completely absent between 52-47 ka BP. At 46 ka BP, the sea ice started to expand again and was occasionally present until MIS 2 when a duration of 1 month/year is estimated between 27 and 17 ka BP. Sea ice then quickly retreated and was absent from the core location since 14 ka BP, except for one short event centred at ~10 ka BP.

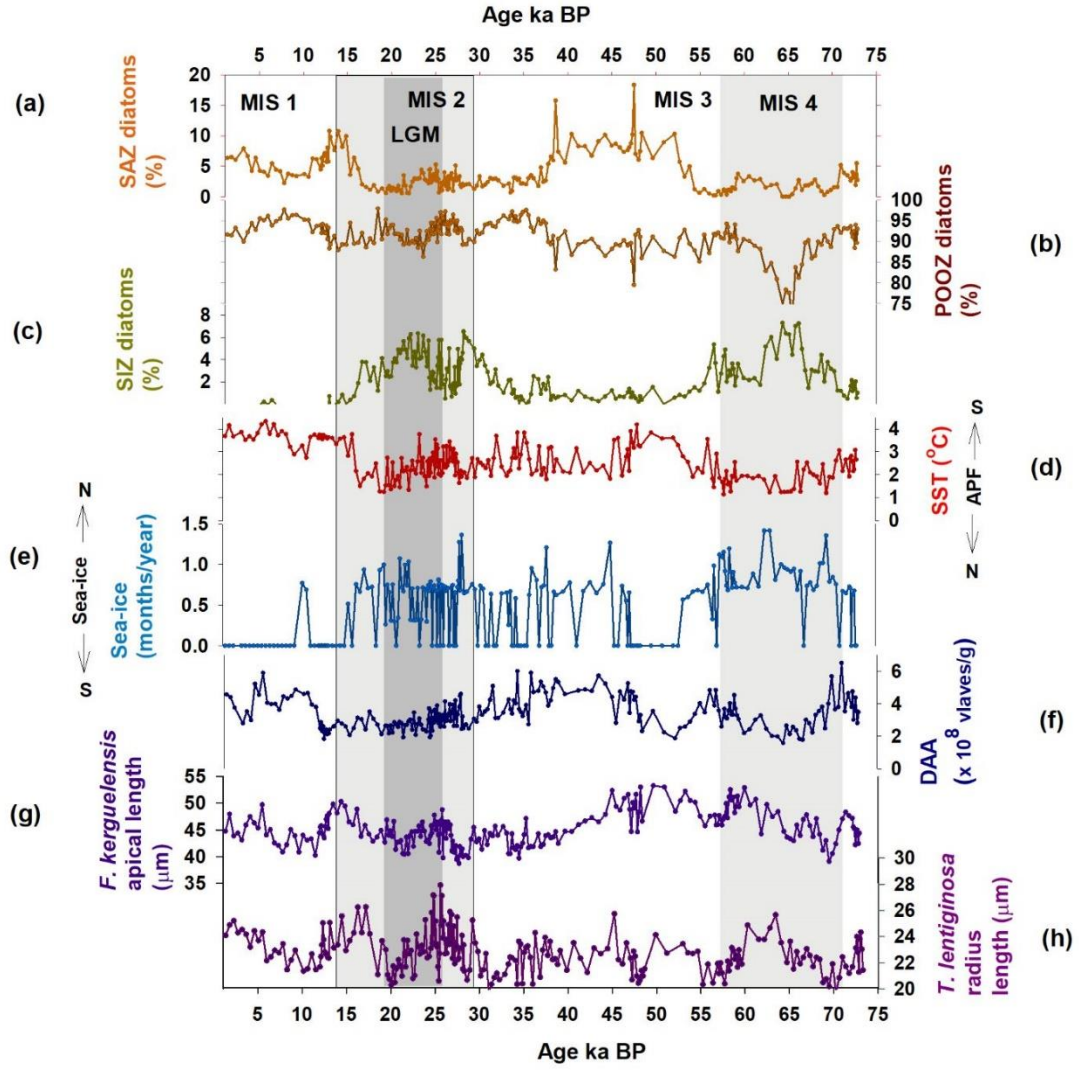

Figure 3: SK 200/27 sediment records a) relative percentage (%) of Sub-Antarctic Zone diatom group (%), b) permanent open ocean zone diatom group (%), c) Sea ice diatom group (%), d) Summer SST, e) Sea-ice duration (months/year), f) DAA, g) *F. kerguelensis* average apical length and h) *T. lentiginosa* radius.

The diatom concentrations at the APF core site, varied between ~2×10^8 and ~6×10^8 valves/g (Fig 3f). Diatom abundances were highest (~6×10^8 valves/g) during early MIS4, mid-late MIS 3 and MIS 1 while lowest concentration (2-3×10^8 valves/g) occurred during late MIS 4, early MIS 3 and MIS 2.

The diatom valve size measurement reveals that the mean apical length of *F. kerguelensis* varied between 40 µm and 54 µm (Fig 3g & Fig 4). The mean apical length increased from MIS 4 (~40 µm) until the early MIS 3 to reach maximum size at ~50 ka BP, then subsequently decreased until MIS 2 when it stabilized at ~43 µm. There was a brief increase in *F. kerguelensis* mean length during the deglaciation (~50 µm), followed by a decrease during the Early Holocene (~43 µm) and an increase during the Late Holocene (~46 µm). Overall the larger valve sizes of *F. kerguelensis* were found during MIS 3 and smaller sizes were found during MIS 2. *Thalassiosira lentiginosa* radius variations in the APF core oscillate between 20 µm and 28 µm with less climate signal. Indeed, both small and large populations are found in each MIS. Sizes of *T. lentiginosa* were larger during MIS 1 and MIS 2, in fact during MIS 2 *T. lentiginosa* had larger size range (Fig 3h & 4).

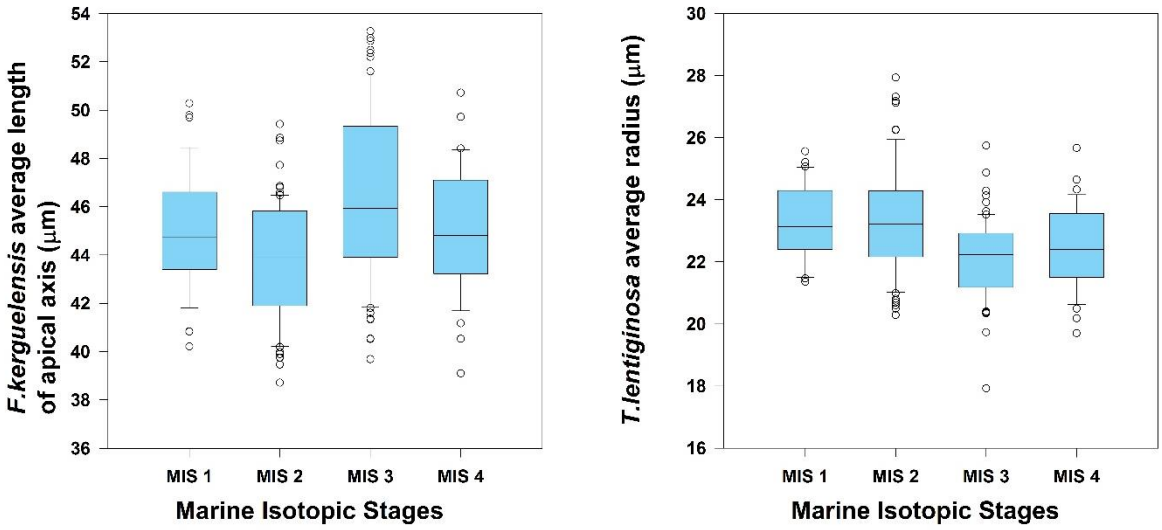

Figure 4: Box plot showing size variation of *F. kerguelensis* and *T. lentiginosa* during MIS 1-4 in SK 200/27.

4.4. Discussion: Latitudinal changes in the Southern Ocean fronts and sea ice extent

Cores SK200/27 is located north of the modern APF northern branch and SK/220/22a positioned below SAF (Chapter 2, Fig 1). Although we are aware that other definitions are existing (Orsi et al., 1995; Belkin and Gordon, 1996: Sokolov & Rintoul, 2009), both fronts can be tracked by strong SST gradients between 3-5°C for the APF and 5-9°C for the SAF in our study area (Lutjerhmas and Valentine, 1984). We subsequently used this relationship, along with variations in the ecological diatom groups and diatom biometry, whereby largest *F. kerguelensis* and *T. lentiginosa* are today found at around the APF (Cortese and Gersonde, 2007; Shukla et al., 2016), to document their past latitudinal shifts.

4.4.1. SST and sea ice duration records

Additionally, the diatom-based transfer function quantifies a ~2°C glacial cooling at both core sites with summer SST around 1-2°C in core SK200/27 (Fig 3d) and 2-3°C in core SK200/22a (Fig 1d). Additionally, the relative abundances of the POOZ diatoms decreased in the APF core SK200/27 (Fig 3b) during the MIS 2 and MIS 4 while they increased in the SAF core SK200/22a (Fig 1b). More specifically, relative abundances of POOZ diatoms in core SK200/22a during glacial times (~90%) were similar to POOZ diatoms relative abundances in core SK200/27 during interglacial times (Fig 1b & 3b). These data suggest an expansion of the ACC. We propose that the APF migrated north during MIS 2 and MIS 4 to reach core site SK200/22a, which represents a shift of 7-8^{o} of latitude relative to its present location. Our results are in agreement with previous studies focusing on the LGM (Gersonde et al., 2005) and add new information on an under-sampled area of the Indian sector of Southern Ocean. Our SST and diatom group data do not show any significant difference between MIS 4 and MIS 2, which suggests that similar conditions may have existed during both glacial periods. Though it is here impossible to track the position of the SAF during glacial times, our data demonstrate a large drop in SAZ diatoms in both cores during glacial times (Fig. 1a & 3a) suggesting a northward migration of the SAF by few degrees of latitude. The northward migration of both the APF and SAF during the glacial periods of the last climatic cycle was probably accompanied by a shift of the ACC (Mazaud

et al., 2010). The shift in the position of ACC (inferred from SAF and APF frontal position) during glacial-interglacial coincides with growth and decay of Antarctic cryosphere and changes in the Southern Hemisphere westerly wind belt probably indicating their role in meridional variation in ACC (Carter and Cortese, 2009).

Both SK 200/22a and SK 200/27 sediment cores are located north of the present winter sea ice edge (Chapter 2, Fig 1). Sea ice records are therefore discontinuous and show the presence of sea ice during glacial times only. The occurrence of sea ice related diatom species (Fig 1c) along with ~ 1 month per year sea ice estimates (Fig. 1e) suggest the presence of episodic and unconsolidated winter sea ice as north as ~43°S during the LGM. Whereas, MIS 4, MIS 3, early MIS 2 and MIS 1 could be characterised by the absence of sea ice at SAF core site. We however assume that the mean winter sea ice limit was located close to APF core site (SK200/27) location during glacial periods, in agreement with previous studies focusing on the LGM (Gersonde et al., 2005). Here again our data suggest that winter sea-ice expansion was similar in MIS 4 than in MIS 2.

Winter sea-ice expansion at glacial inceptions and shrinking at deglaciations appear very abrupt suggesting a strong sensitivity to oceanographic and climate changes (Crosta et al., 2004; Ferry et al., 2015). The northward expansion of sea ice during the glacial periods is associated with the Antarctic ice sheets extension (probably as a result of changes in Antarctic temperature) and equator displacement of Southern Hemisphere westerlies (Neil et al., 2004; Carter and Cortese, 2009; Martinson, 2012; Kohfeld et al., 2013), suggesting a close link between Antarctica and Southern Ocean.

4.4.2. Records of diatom absolute abundance

Diatom productivity, here tracked through diatom absolute abundances, shows a distinct glacial-interglacial variation in both cores (Fig 5b and d). The SAF core site was characterised by higher diatom productivity during glacial period, which resulted in increased TOC and opal content in glacial sediments (Manoj and Thamban, 2015: Nair et al., 2015).

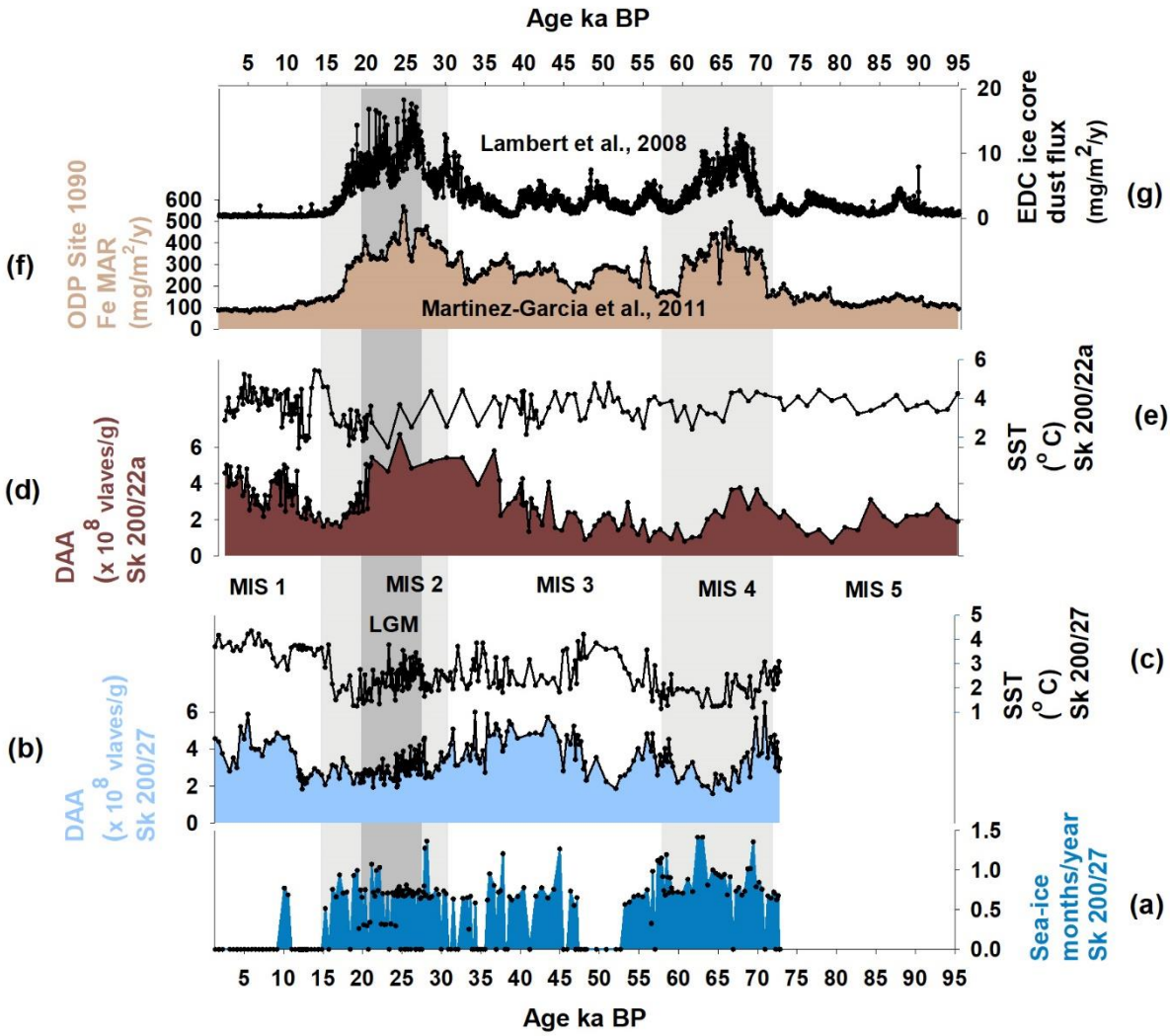

Figure 5: Diatom productivity variation and comparison: a) SK 200/27 sea ice records, b) SK 200/27 DAA, c) SST SK 200/27, d) SK 200/22a DAA, e) SST SK 200/22a, f) Fe MAR (Martinez-Garcia et al., 2011) and g) EDC dust flux (Lambert et al., 2008).

Higher diatom productivity during glacial period at core site SK200/22a may have been driven by increased supply of Si to the SAZ surface water in response to the northward migration of APF and Southern Ocean upwelling (Sigman and Boyle, 2000; Anderson et al., 2002; Dezileau et al., 2003; Sigman et al., 2010). An increased dust flux (Fig 5f) to the SO from South America and South Africa (Lamy et al., 2014) may have also contributed to the observed glacial rise in siliceous productivity both in the SAZ Atlantic (Kumar et al., 1995; Frank et al., 2000; Anderson et al., 2002; Jaccard et al., 2013) and SAZ Indian (Bareille et al., 1998; Dezileau et al., 2003; Nair et al., 2015).

Conversely, diatom productivity was reduced at the APF core site during MIS 2 and MIS 4 compared to the Holocene. This drop in siliceous productivity may result from the northward migration of the Southern Ocean upwelling and enhanced stratification in the POOZ due to longer sea-ice duration at core site SK 200/27. Indeed, the enhanced sea-ice cycle during the glacial periods (Gersonde et al., 2005) may have allowed a low salinity lid to accumulate in the POOZ (Shin et al., 2003), thus reducing the vertical mixing and associated vertical supply of nutrients (François et al., 1997; Crosta and Shemesh, 2002; Jaccard et al., 2013). Additionally, the greater sea-ice cover may have reduced the length of the growing season (Moore et al., 2000) and favoured smaller sea ice related diatoms at the expense of large POOZ diatoms.

4.4.3. Size records of *F. kerguelensis* and *T. lentiginosa*

Earlier studies have shown that larger F. kerguelensis and T. lentiginosa valves occur in modern sediments underlying the APF (Cortese et al., 2007; Shukla et al., 2016) where favourable SST of 3-5°C allow them to make use of the high nutrient content in turbulent waters of the frontal system. Building on these findings we used downcore variations in *F. kerguelensis* and *T. lentiginosa* size to further document past meridional shifts in the APF. Glacial summer SST of 2-3°C (Fig. 1d) along with larger mean size of both diatom species (Fig 1g and h) recorded at the SAF core site support the northward migration of the hydrological fronts and place the glacial APF at around 43°S. Glacial summer SST of 2-3°C (Fig. 1d) along with larger mean size of both diatom species (Fig 1g and h) recorded at the SAF core site support the northward migration of the hydrological fronts and place the glacial APF at around 43°S. Both *F. kerguelensis* and *T. lentiginosa* were then at their optimal ecological range (Crosta et al., 2005), silica standing stocks were probably higher due to the migration of the Southern Ocean upwelling along with the ACC and fronts (Sigman et al., 2000) and higher iron concentrations injected by the upwelling and aeolian dust (Lamy et al., 2014) may have allowed the diatoms to grow larger initial cells (Assmy et al., 2006).

Conversely, smaller mean sizes of *F. kerguelensis* and *T. lentiginosa* are observed at the APF core site during the MIS 4 and MIS 2 periods compared to

interglacial periods (Fig 3 g and h). Smaller diatoms in the POOZ during glacial times probably resulted from summer SST below 2-3°C (Fig. 3d) that are out of the preferred ecological range of these species (Crosta et al., 2005), episodic presence of sea-ice over the core site (Fig. 3e; Gersonde et al., 2005) and reduced nutrient stocks due to water column stratification (François et al., 1997; Crosta and Shemesh, 2002; Jaccard et al., 2013). Although growth rate and, thus, size reduction were dampened, unfavourable SST may have prevented diatoms to make full use of the low silica stocks to develop large initial cell. As such the diatom communities during glacial times probably developed smaller initial cells (Crosta, 2009).

4.5. Conclusion

1. SAF core site records the presence of episodic and unconsolidated winter sea ice as north as ~43°S during the LGM. We however believe that the mean winter sea ice limit was located close to core modern day APF (SK200/27) location during the glacial periods.
2. Higher diatom productivity during glacial periods at SAF suggest northward shift of APF with the corresponding decrease in glacial diatom productivity at modern APF highlighting stratified POOZ due to longer sea ice presence.
3. Larger average sizes of *F. kerguelensis* and *T. lentiginosa* at the SAF core site during glacial period support the concept of northward migration of the hydrological fronts wherein the glacial APF was positioned at around 43°S. While, smaller mean sizes of *F. kerguelensis* and *T. lentiginosa* are at the APF core site during the MIS 4 and MIS 2 periods compared to interglacial periods suggest a more stratified and cooler POOZ during glacial period indicating the winter sea ice presence.

Chapter 5

Comparison of Southern Ocean data with other climatic records

5.1. Linkages between Southern Hemisphere high-latitude and Asian summer monsoon for the last 500 ka BP

5.1.1. Background

Changes in Southern Hemisphere high latitude temperature and sea ice have been previously shown to influence meridional displacements in the Intertropical Convergent Zone (ITCZ) and Asian monsoon system (Chiang and Bitz, 2005; An et al., 2011; Caley et al., 2013). The impact of Antarctic temperature changes on the Asian summer monsoon is mainly through changes in atmospheric pressure difference between the Asian low and the Mascarene High in the southern Indian Ocean thereby influencing the cross-equatorial pressure gradient (An et al., 2011). As evident from tropical paleo-data, there is substantial evidence for robust coupling between Northern high-latitude temperature changes and tropical precipitation shifts (Peterson et al. 2000; Wang et al. 2001, 2008; Lea et al. 2003; Koutavas and Sachs 2008; Dubois et al. 2011). However, the recorded precipitation shifts are not likely to be influenced by northern-only or southern-only high-latitude changes. It is more probable that they disclose an intricate interaction between Northern and Southern Hemisphere high-latitude climate shifts as suggested by Rohling et al. (2009) and Kanner et al. (2012). In this chapter we provide a broad comparison between Southern Hemisphere high-latitude records (SO SSTs and Antarctic temperature), Southern Indian Ocean subtropical records (Agulhas leakage) and Asian summer monsoon records for the last 500 ka BP. Such comparative study on a longer timescale would allow us to better understand the interaction between Southern Hemisphere high-latitude, subtropics and Asian Monsoon.

5.1.2. Supporting data

To understand the linkages between Southern Hemisphere high-latitude and Asian summer monsoon we used SST records from Atlantic and Indian Sector of SO (Crosta et al., 2004; Cortese et al., 2007; Martinez et al., 2009), Antarctic atmospheric temperature- EPICA Dome C (EDC) ice core temperature estimates (Jouzel et al., 2007), Agulhas leakage fauna (ALF, Peeters et al., 2004; Simon et al., 2013), Asian monsoon records such as Arabian sea Sediment total reflectance (Deplazes et al., 2013), ^{10}Be-proxy rainfall records (Beck et al., 2018), Chinese

Hulu and Dongge Cave stalagmite records $\delta^{18}O$ (Wang et al., 2001; Yuan et al., 2004), 30°N to 30°S June insolation difference (Berger and Loutre, 1991). The locations of the supporting dataset are shown in figure 1.

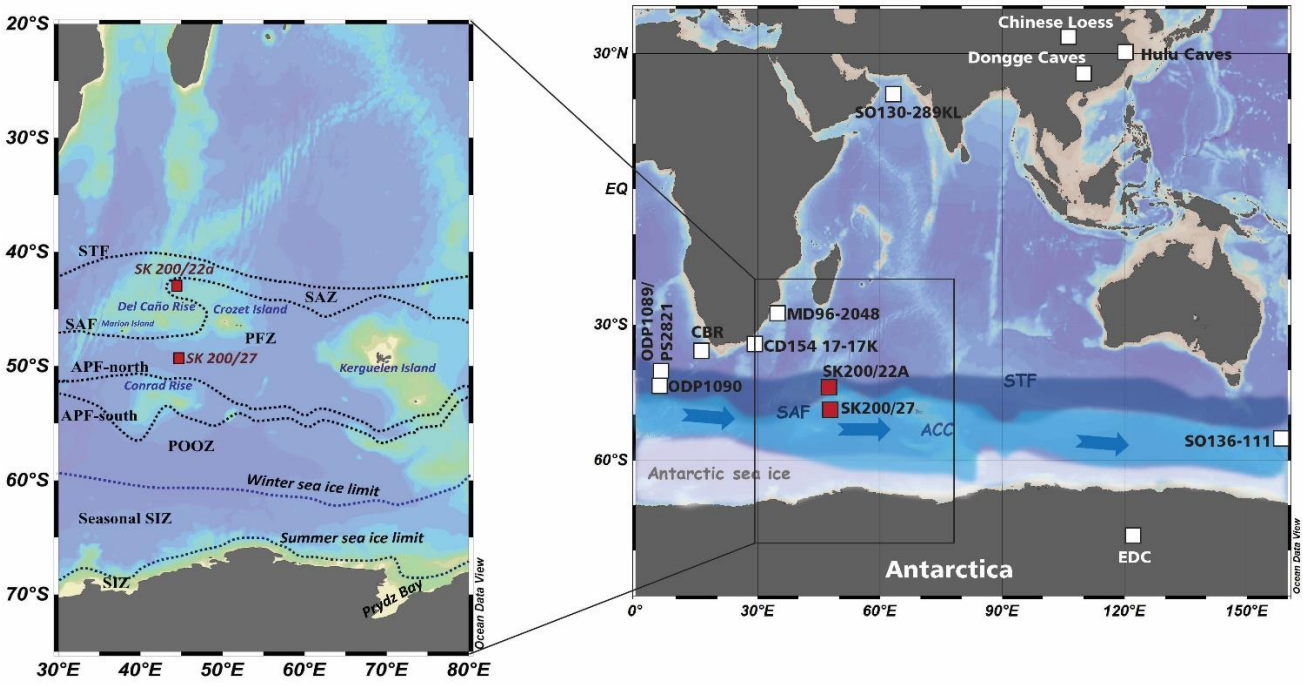

Figure 1: The map shows the location of sediment cores SK 200/22a and SK 200/27 (red boxes) along with location of the supporting dataset (white boxes). The positions of the Subtropical Front (STF), Sub-Antarctic Front (SAF), Polar Front (APF), and winter sea ice limit based on (Belkin and Gordon, 1996; Orsi et al. 1995; Comiso, 2003; Pollard and Read, 2001; Pollard et al., 2007: Sokolov & Rintoul 2009 a, b). Schematic view of the location of the core sites SK200/22a and SK200/27.

5.1.3. Discussion

Studies in the past have suggested a prominent Northern Hemisphere control on Asian summer monsoon dynamics on a suborbital to millennial timescale (Schulz et al., 1998; Wang et al., 2001; Altabet et al., 2002; Burns et al., 2003; Rohling et al., 2003; Yuan et al., 2004; Ivanochko et al., 2005; Cosford et al., 2008; Deplazes et al., 2013). These studies were based on the apparent resemblance of Indo-Asian records with those of Greenland $\delta^{18}O$ ice-core records (NGRIP members, 2004) at millennial/suborbital scale. However, a recent study has argued that the Asian summer monsoon is governed by the low-latitude (30°N-30°S) interhemispheric insolation gradient rather than high-northern-latitude isolation (Beck et al., 2018). Likewise, only few studies have suggested teleconnections

between Asian monsoon and the regions other than Northern Hemisphere (An et al., 2011; Caley et al., 2013; Gebregiorgis et al., 2018). Modern observations suggested that it is the differential heating between the hemispheres at low-latitude which controls the tropical monsoon build-up (Webster, 2005; Beck et al., 2018). Asian monsoon is linked to southern Indian Ocean subtropical high (SISH)/Mascarene High and North Pacific subtropical high through Hadley circulation and walker circulation pathways respectively (Beck et al., 2018). Present day observations indicated that the changes in the strength and position of SISH is coupled with the Agulhas Current (AC) strength and leakage (Beck et al., 2018; Backeberg et al., 2012), which is also influenced by Southern Hemisphere high latitude forcing through changes in STF position (Caley et al., 2011). Hence to understand the linkages between Southern Hemisphere high-latitude changes and Asian summer monsoon we made a comparison between the SST records from SO, Antarctic paleotemperature, Agulhas leakage, Asian summer monsoon records and low-latitude insolation gradient (June 30°N to 30°S) for the last 500 ka BP (Fig 2).

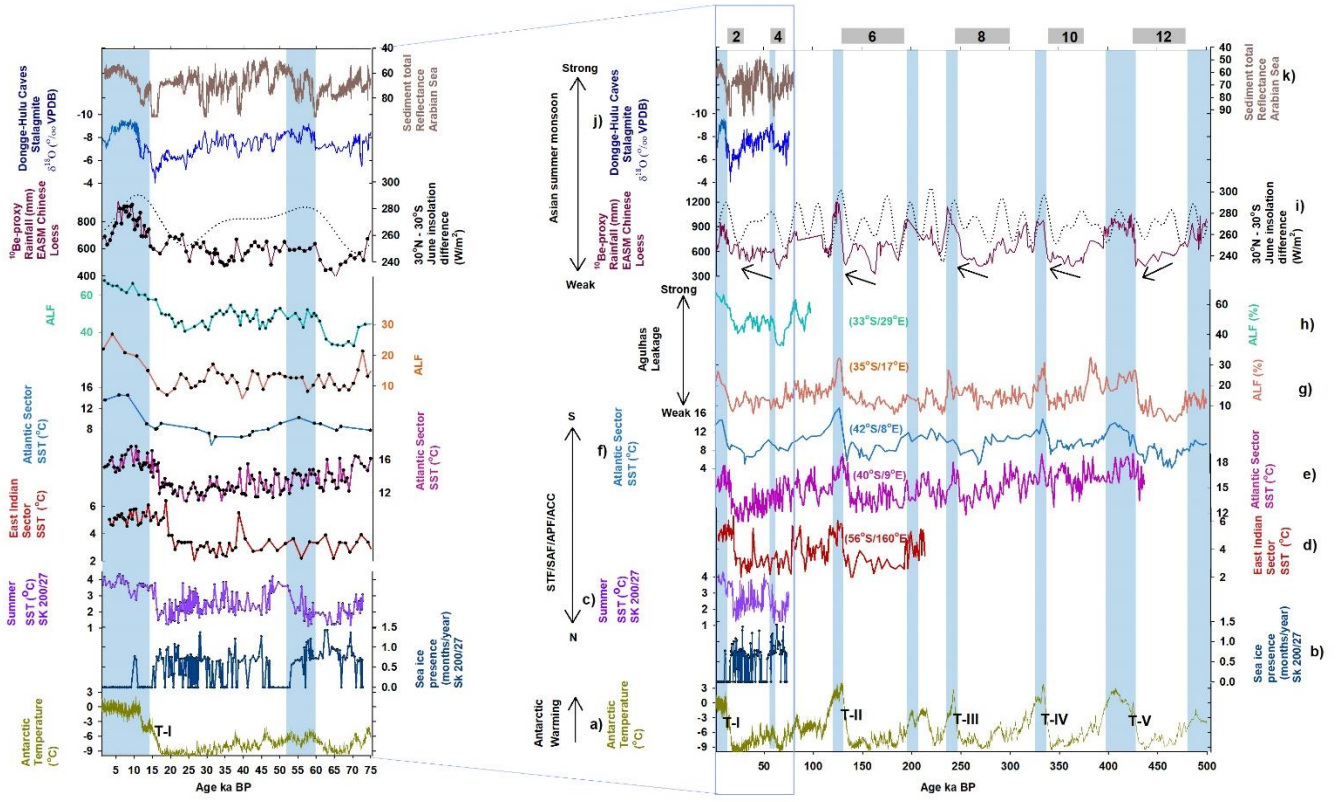

Figure 2: Comparison between records of Southern Hemisphere High-latitude, Southern Indian Ocean subtropics and Asian summer monsoon. (a) Antarctic atmospheric

temperature- EPICA Dome C (EDC) ice core, (b) SK 200/27 sea ice duration, (c) SK 200/27 SST, (d) SST from East Indian Sector of SO (Crosta et al., 2004), (e) SST from SO Atlantic STF (Cortese et al., 2007), (f) SST from SO Atlantic SAZ (Martinez et al., 2009), (g) Agulhas leakage fauna (Peeters et al., 2004), (h) Agulhas leakage fauna (Simon et al., 2013), (i) ^{10}Be-proxy rainfall records and 30°N to 30°S June insolation difference (dotted curve), (j) Hulu and Dongge Cave stalagmite records δ^{18}O and (k) Arabian sea Sediment total reflectance. The light blue bands indicate periods of increased Asian summer monsoon and the black arrows shows the trend in Asian summer monsoon within the glacial periods (grey boxes with MIS stages).

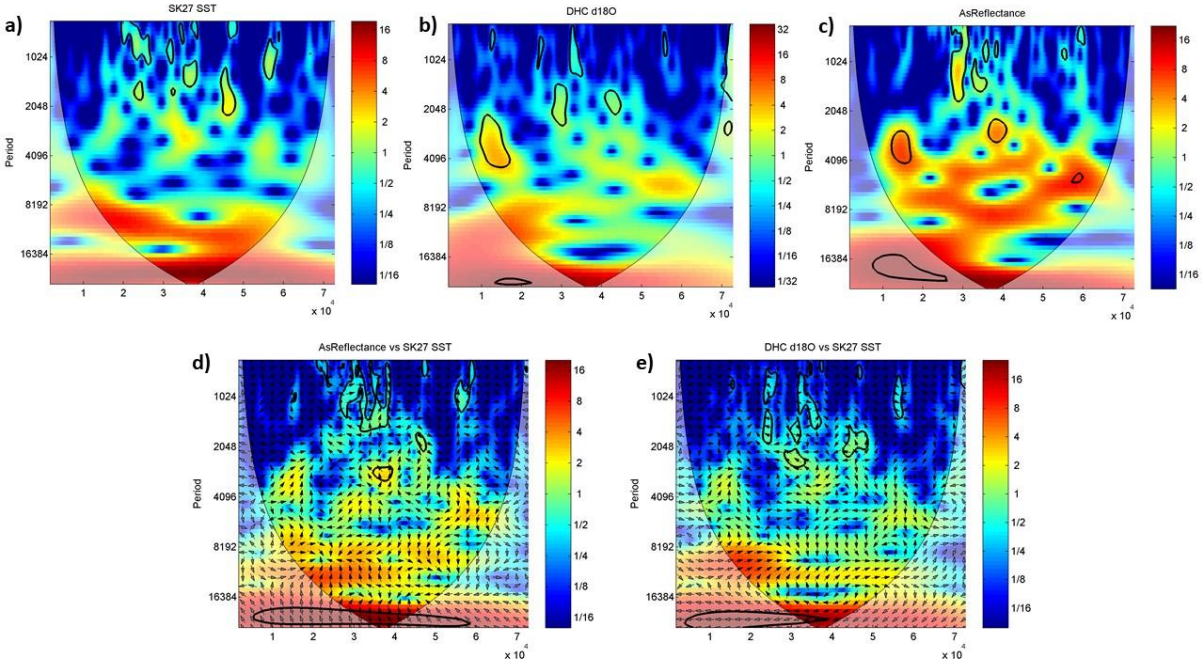

Figure 3: Wavelet analysis a) SK 200/27, b) δ^{18}O stalagmite Hulu (Wang et al., 2001) and Dongge caves (Yuann et al., 2004), c) Reflectance L* from the Arabian Sea (Deplazes et al., 2013), Cross-wavelet analysis d) SK 200/27 v/s Reflectance L* from the Arabian Sea and e) SK 200/27 v/s δ^{18}O stalagmite Hulu and Dongge caves.

Changes in East Asian summer monsoon as indicated by the ^{10}Be records exhibit a strong match with the low latitude (30°N to 30°S) June insolation gradient (Fig 2i) suggesting a precession driven forcing for the last 500 ka BP (Beck et al., 2018). Such low latitude insolation forcing on Asian summer monsoon is also evident from the precession scale periodicities obtained through the wavelet analysis of Dongge-Hulu cave δ^{18}O and Arabian Sea reflectance records for last 75 ka BP (Fig 3b and c). The Asian monsoon dynamics for the last 500 ka BP revealed stronger monsoon during the past interglacial periods. This can be explained by the fact that the stronger cross-equatorial flow of South-East (SE) trade winds and Somali Jet, when the gradient of June isolation between 30°N-30°S, was maximum along with the stronger low pressure over Asian landmass (Beck et al., 2018).

Modern observations (Backeberg et al., 2012) have suggested that, with the intensification of SE trade winds there is a resultant increase in the wind stress coupling to the sea surface thereby leading to enhanced South Equatorial Current (SEC) and strengthened AC in the south west Indian Ocean. These observations have further indicated increased Agulhas leakage with the strengthened AC intensity (Fig 4a). Likewise, the observed similarity between the ALF (Fig 2h and g), Asian summer monsoon variation (Fig 2i) during the past interglacial periods may indicate increased Agulhas leakage in to the Atlantic Sector as a result of upstream changes in Agulhas system. Wherein AC was strengthened and fed by intensified SEC (caused by stronger SE trade winds) during stronger Asian summer monsoon (Fig 4a; Peeters et al., 2004). Increased Agulhas leakage during interglacial period might have been further assisted by southward position of SO fronts, widening the Agulhas leakage corridor, as indicated by higher SO SST (Fig 2c, d, e and f) regulated by increased Antarctic temperature (Fig 2a).

Contrastingly, during the past glacial periods, the minimum gradient of June isolation between 30°N-30°S (causing weak cross-equatorial pressure gradient between SISH and Asian landmass) might have led to decreased cross-equatorial flow of SE trade wind and Somali jet lowering the Asian summer monsoon intensity (Beck et al., 2018). However, Asian monsoon intensity exhibited a gradual increasing trend during the past glacial periods (except MIS 12). Such non-orbital scale variation could be attributed to cooler and stronger SISH, leading to increased pressure gradient between SISH and Asian Low (however this pressure gradient is still weaker than that observed during interglacials), due to SO and Antarctic cooling (Fig 2i; An et al., 2011). This glacial scenario (of low monsoon intensity) might have led to the weakened flow of AC (due to weaker SEC) coupled with more northward position of SO fronts (narrowing of the Agulhas leakage corridor) thereby resulted in the reduced Agulhas leakage (Fig 4c). Additionally, during the glacial periods, the increased strength of Agulhas return current (ARC) due to intensified Southern Hemisphere westerlies (ARC, Simon et al., 2013) coupled with reduced Agulhas leakage could lead to the build-up of heat that could not escape to the Atlantic. Such scenario could possibly lead to warmer SST anomaly (specially seen during MIS 12 in Caley et al., 2011) in south west Indian Ocean during the glacial period which might further weaken the SISH and thus

additionally contribute in lowering the Asian summer monsoon intensity during glacial periods (Fig 4b). Warmer SST anomaly during MIS 12 glacial period in the south west Indian Ocean (Caley et al., 2011) could be a possible explanation for the decreased trend in Asian summer monsoon (Fig 2i), through weakened SISH, observed during the same period, which otherwise displays an increased trend during glacial period as observed by An et al, (2011). It would be interesting to look for such anomalies in SST variation in SISH region, where records are lacking, during glacial periods given the increased heat build-up due to reduced Agulhas leakage conditions.

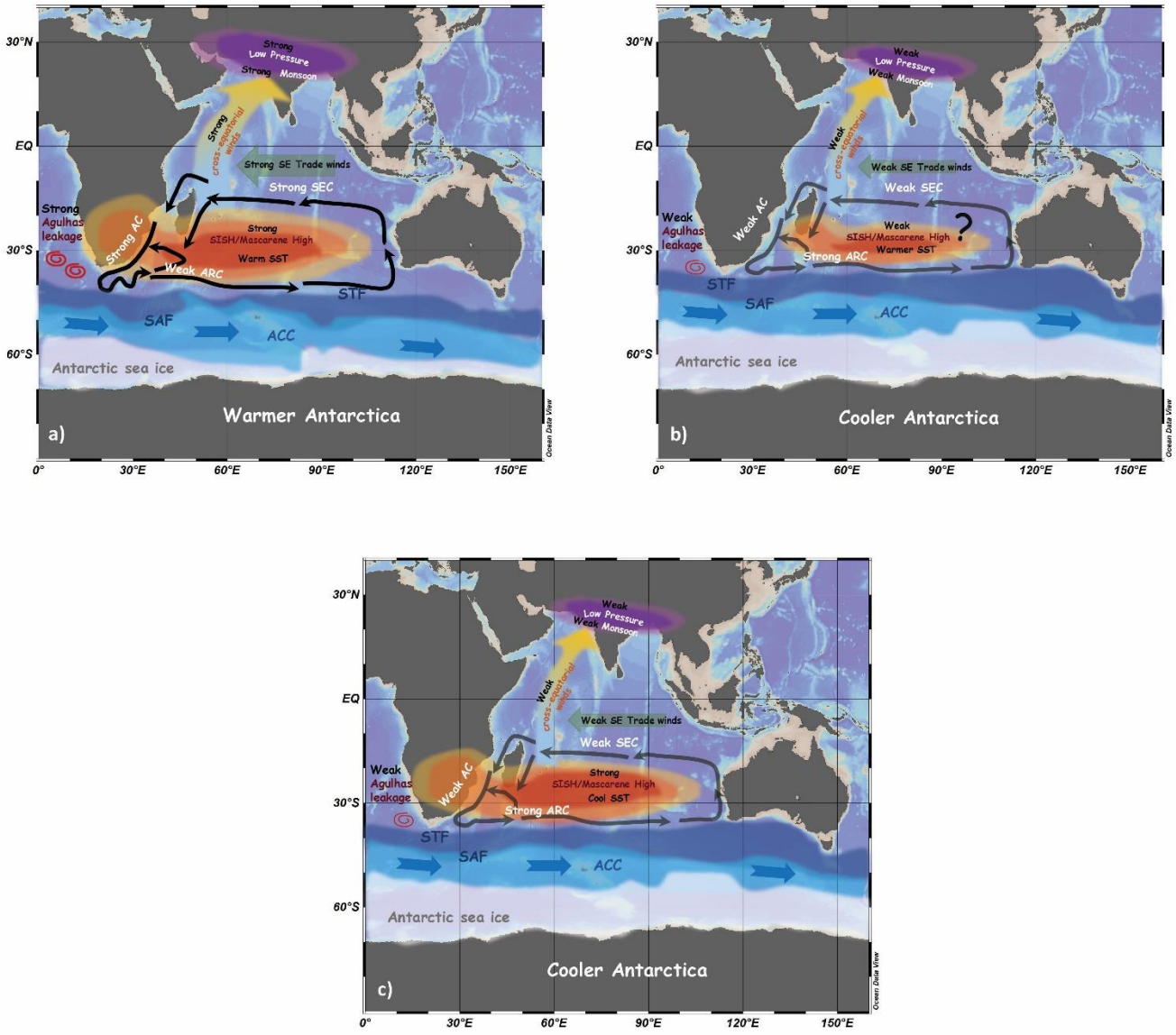

Figure 4: Different scenarios showing changes in the Southern Hemisphere high latitude, Southern Indian Ocean subtropics and Asian summer monsoon during (a) interglacial periods and terminations, (b & c) glacial periods. The Antarctic sea ice and frontal positions during

the glacial periods are marked referring to LGM location of the sea ice and fronts provided by Gersonde et al. (2005) and Bostock et al. (2013).

Our assumption on the glacial-interglacial variation in the AC strength and Agulhas leakage is different from that of Caley et al, (2011). Which suggested that the stronger Agulhas current during glacial periods led to reduced Agulhas leakage. This is primarily associated with northward STF and westerlies position as a result of Southern Hemisphere high-latitude forcing rather than low-latitude monsoon control (Caley et al., 2011). However, the Southern Hemisphere high latitude forcing on AC and Agulhas leakage is still debatable. This is because Simon et al, (2013) suggested that the changes in SST and salinity in the Agulhas leakage corridor may be partly induced via upstream variations in these properties within the source region of Agulhas leakage. Hence it is probably the changes in low latitude (Asian monsoon) along with the meridional variation SO fronts which could explain the Agulhas leakage variability in the past.

The main driver of Asian monsoon for the last 500 ka BP is suggested to be precession forcing via low latitude insolation (Beck et al., 2018), whereas Gebregiorgis et al, (2018) highlighted the sensitivity of the Asian summer monsoon to internal processes that are associated with the precession, obliquity and eccentricity band forcing. However, the scenario of intensified Asian summer monsoon during periods of decreased obliquity forcing (Gebregiorgis et al., 2018) was not evident through the comparison made between Beck et al, (2018) monsoon records and obliquity (Fig 5b, d). The ~100 ka eccentricity cycle in the monsoon records were attributed to the basin isolation and monsoon intensification induced by sea level changes (Fig 5b, c; Gebregiorgis et al., 2018).

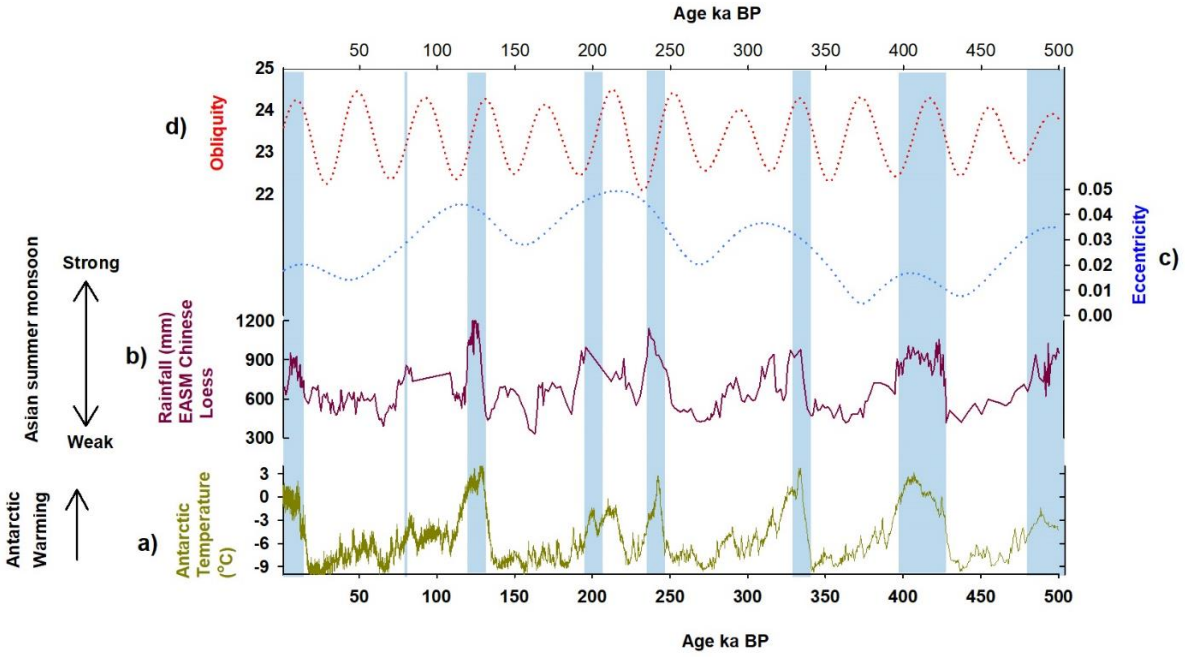

Figure 5: Comparison of (a) Antarctic temperature, (b) ^{10}Be-proxy rainfall records, (c) Eccentricity and (d) Obliquity (Berger and Loutre, 1991).

5.1.4. Conclusion

The variability of the Asian summer monsoon for the past 500 ka BP could be more likely forced by low latitude (30°N-30°S) insolation gradient. However, changes in the Asian summer monsoon intensity on a non-orbital scale could have been forced by the Southern Hemisphere high-latitude (Antarctic) climate changes (An et al., 2011). Variation in the intensity of the Asian summer monsoon in the past could have influenced the Sothern Indian Ocean subtropical gyre through changes in SEC and AC strength. This changes in circulation in turn might have had a feedback effect on Asian summer monsoon via Agulhas leakage.

Chapter 6

Conclusion and summary

6: Conclusion and summary

This PhD study produced numerous new diatom bound records from the Indian sector of Southern Ocean (understudied) and provide fresh understandings of the variations and changes in the climate and environment in the Southern Ocean during the late Quaternary.

The records recovered from Del Cano Rise region sector of Southern Ocean offer wide-ranging knowledge for the climate reconstruction in the Western Indian sector of Southern Ocean for the past 95 ka (Chapter 4). Age model for the two sediment cores have been established through AMS ^{14}C dating and correlation of the stable isotope and geochemical profiles of the cores with the stacked oceanic and ice core records from Southern Hemisphere (Chapter 2). The diatom-based transfer function quantifies a ~2°C glacial cooling at both core sites with summer SST around 1-2°C in core SK200/27 and 2-3°C in core SK200/22a (Chapter 4). The SAF core site also archives the presence of episodic and unconsolidated winter sea ice as north as ~43°S during the LGM. We however believe that the mean winter sea ice limit was located close to APF core SK200/27 location during the glacial periods (Chapter 4). This is also backed by the increase in diatom productivity during glacial periods at SAF, suggesting northward shift of APF with the corresponding decrease in glacial diatom productivity at modern APF highlighting stratified POOZ due to longer sea ice presence (Chapter 4). Additionally, diatom morphometry indicated larger average sizes of *F. kerguelensis* and *T. lentiginosa* at the SAF core site during glacial period, supporting the northward migration of the hydrological fronts wherein the glacial APF was positioned at around 43°S. However, smaller sized *F. kerguelensis* and *T. lentiginosa* were at the APF core site during the MIS 4 and MIS 2 periods compared to interglacial periods suggesting a more stratified and cooler POOZ during glacial period indicating winter sea ice presence.

The comparative study of various records revealed a complex interaction between Southern Hemisphere high-latitude, southern Indian Ocean subtropics and Asian summer monsoon (Chapter 5). Southern Hemisphere high-latitude (Antarctica) climate changes via meridional shifts in the position of the fronts and sea ice explains much of the non-orbital scale variance in Asian summer monsoon.

However, the low latitude insolation gradient is the main forcing factor for the variability of the Asian summer monsoon for the last 500 ka BP. The past changes in the intensity of Asian summer monsoon might have influenced the Sothern Indian Ocean surface circulation (SEC and AC strength). Whereas, Asian summer monsoon along with SO frontal variation might be responsible for the changes in the Agulhas leakage intensity in the past.

The western Indian sector of Southern Ocean is important area for studying and perceiving the climate dynamics owing to its location close to Mascarene high in southern Indian Ocean which is a vital region in context of Asian summer monsoon. Thus, the sea ice distribution and oceanic frontal system in the Western Indian sector of South Ocean which is nearly linked to the Antarctic ice sheet dynamics and Southern Hemisphere westerly wind system can impact the Asian summer monsoon. In future it is imperative to retrieve longer sediment core records and have quantitative reconstruction from the Masacarene high, Central Indian Ocean and Indian sector of Southern Ocean. This is to better understand the interaction between Southern Ocean, Southern Indian Ocean subtropical gyre and Asian monsoon. Such records will aid to provide a broader picture of the climate change in Southern Ocean and its interaction with other climate system.

References

Abelmann, A., Gersonde, R., 1991. Biosiliceous particle flux in the Southern Ocean. Marine Chemistry, 35, 503– 536.

Abelmann, A., Gersonde, R., Cortese, G., Kuhn, G., Smetacek, V., 2006. Extensive phytoplankton blooms in the Atlantic sector of the glacial Southern Ocean. Paleoceanography 21, PA1013, doi: 10.1029/2005PA001199.

Abelmann, A., Gersonde, R., Knorr, G., Zhang, X., Chapligin, B., Maier, E., Esper, O., Friedrichsen, H., Lohmann, G., Meyer, H. &Tiedemann, R. 2015. The seasonal sea-ice zone in the glacial Southern Ocean as a carbon sink. Nature Communications, 6, 10.1038/ncomms9136.

Ackley, S. F., A. J. Gow, K. R. Buck, K. M. Golden. 1980. Sea ice studies in the Weddell Sea aboard USCGC Polar Sea. Antarctic Journal of the United States, 15, 5, 84-96.

Akiba, F., 1982. Late Quaternary diatom biostratigraphy of the Bellingshausen Sea, Antarctic Ocean. Report of the Technology Research Centre, J.N.O.C. 16, 31– 74.

Altabet, M. A., Higginson, M. J., and Murray, D. W., 2002.The effect of millennial-scale changes in Arabian Sea denitrification on atmospheric CO_2, Nature, 415, 159–162

Anderson, J.B., 1999. Antarctic Marine Geology. Cambridge University Press, Cambridge, 289pp.

Anderson, J., Shipp, S., Lowe, A., Wellner, J.S., Mosola, A., 2002. The Antarctic Ice Sheet during the last glacial maximum and its subsequent retreat history: a review. Quaternary Science Reviews, 21, 49-70.

Anderson, R.F., Ali, S., Bradtmiller, L.I., Nielsen, S.H.H., Fleisher, M.Q., Anderson, B.E., Burckle, L.H., 2009. Wind driven upwelling in the Southern Ocean and the deglacial rise in atmospheric CO2. Science, 323, 1143-1148.

Anderson, R.F. and Carr, M. E., 2010. Uncorking the Southern Ocean's vintage CO_2. Science, 328, 1117-1118.

An, Z., Clemens, S.C., Shen, J., Qiang, X., Jin, Z., Sun, Y., Prell, W.L., Luo, J., Wang, S., Xu, H., Cai, Y., Zhou, W., Liu, X., Liu, W., Shi, Z., Yan, L., Xiao, X., Chang, H., Wu, F., Ai, L., Lu, F., 2011. Glacial-Interglacial Indian summer monsoon dynamics. Science 333, 719e723. http://dx.doi.org/10.1126/science.1203752.

Armand, L., Crosta, X., Romero, O., & Pichon, J. J. (2005). The biogeography of major diatom taxa in Southern Ocean sediments. 1. Sea-ice related species. Palaeogeography, Palaeoclimatology, Palaeoecology, 223, 93–126.

Assmy, P., Henjes, J., Smetacek, V. & Montresor, M. 2006. Auxospore formation by the silica-sinking, oceanic diatom Fragilariopsis kerguelensis (Bacillariophyceae). Journal of Phycology, 42, 10.1111/j.1529-8817.2006.00260.x.

Bae, S.H., Yoon, H.I., Park, B.K., 2003. Late Quaternary stable isotope record and meltwater discharge anomaly events to the south of the Antarctic Polar Front, Drake Passage. Geo-Mar. Lett. 23, 110–116. http://dx.doi.org/10.1007/s00367-003-0129-y.

Bard, E., 1988. Correction of accelerator mass spectrometry 14C ages measured in planktonic foraminifera: paleoceanographic implications. Paleoceanography 3, 635‑645.

Bareille, G., Labracherie, M., Bertrand, P., Labeyrie, L., Lavaux, G., Dignan, M., 1998. Glacial–interglacial changes in the accumulation rates of major biogenic components in Southern Indian Ocean sediments. Journal of Marine Systems 17, 527–539.

Barker, P.F., Diekmann, B., Escutia, C., 2007. Onset of Cenozoic Antarctic glaciations. Deep-Sea Research II, 54, 2293-2307.

Barker, P.F. and Thomas, E., 2004. Origin, signature and palaeoclimatic influence of the Antarctic Circumpolar Current. Earth-Science Reviews, 66, 143-162.

Batterby, R.W. 1986. Diatom analysis. In: Berglund, B.E. (Ed), Handbook of Holocene Paleoecology and Paleohydrology, John Wiley, Chichester, U. K. pp. 527–570.

Backeberg, B.C., Penven, P., Rouault, M., 2012. Impact of intensified Indian Ocean winds on mesoscale variability in the Agulhas system. Nature Climate Change, 2 (2012), pp. 608-612.

Beck, J.W., Zhou, W., Li, C., Wu, Z., White, L., Xian, F., Kong, X., An, Z., (2018). A 550,000-year record of East Asian monsoon rainfall from ^{10}Be in loess. Science 360, 877–881.

Belkin, I.M., Gordon, A.L., 1996. Southern Ocean fronts from the Greenwich meridian to Tasmania. J. Geophys. Res. 101, 3675–3696. doi:10.1029/95JC02750.

Berger, A., M. F. Loutre, J. L. Mélice. Equatorial insolation: from precession harmonics to eccentricity frequencies. Climate of the Past, European Geosciences Union (EGU), 2006, 2 (2), pp.131-136.

Berkman, P.A., Forman, S.L., 1996. Pre-bomb radiocarbon and the reservoir correction for calcareous marine species in the Southern Ocean. Geophys. Res. Lett. 23, 363–366.

Bianchi, C. and Gersonde, R., 2004. Climate evolution at the last deglaciation-the role of the Southern Ocean. Earth and Planetary Science Letters, 228, 407-424.

Blunier, T., Brook, E.J., 2001. Timing of millennial-scale climate change in Antarctica and Greenland during the last glacial period. Science 291, 109–112.

Boelhouwers, K., Meiklejohn, K.I., Holness, S.D., Hedding, D.W., 2008. Geology, geomorphology and climate change. In: Chown, S.L., Froneman, P.W. (Eds.), The Prince Edward Islands. Land-sea Interactions in a Changing Ecosystem. Sun Press, Stellenbosch, South Africa, pp. 65-96.

Bostock et al., 2013. A review of the Australian-New Zealand sector of the Southern Ocean over the last 30 ka (Aus-INTIMATE project). Quaternary Science Reviews, 74, 35-57.

Bouttes, N., Roche, D.M., Paillard, D., 2009. Impact of strong deep ocean stratification on the glacial carbon cycle. Paleoceanography, 24, PA3203, doi: 10.1029/2008PA001707.

Brathauer, U., Abelmann, A., Gersonde, R., Niebler, H.-S., Futterer, D.K., 2001. Calibration of *Cycladophora davisiana* events versus oxygen isotope stratigraphy in the subantarctic Atlantic Ocean - a stratigraphic tool for carbonate-poor Quaternary sediments. Marine Geology, 175, 167-181.

Bryden, H.L. and Cunningham, S.A., 2003. How wind forcing and the air-sea heat exchange determine meridional temperature gradient and strati_cation for the Antarctic

Circumpolar Current. Journal of Geophysical Research, 108. doi:10.1029/2001JC001296.

Burckle, L.H. and Burak, R.W., 1988. Fluctuations in Late Quaternary diatom abundances: stratigraphic and paleoclimatic implications from subantarctic deep sea cores. Palaeogeography, Palaeoclimatology, Palaeoecology, 67, 147-156.

Burckle, L.H., Robinson, D., Cooke, D., 1982. Reappraisal of sea-ice distribution in Atlantic and Pacific sectors of the Southern Ocean at 18,000 yr BP. Nature 299, 435–437. Cooke, D.W., 1978. Ph.D. Thesis, Columbia University, New York.

Burckle, L.H., Cirilli, J., 1987a., Origin of the diatom ooze belt in the Southern Ocean: implications for the late Quaternary paleoceanography. Micropaleontology 33 (1), 82–86.

Burckle, L.H., Jacob, S.S., McLaughlin, R.B., 1987b. Late austral spring diatom distribution between New Zealand and the Ross Ice Shelf, Antarctica: hydrography and sediment correlations. Micropaleontology 33 (1), 74– 81.

Burns, S. J., Fleitmann, D., Matter, A., Kramers, J., and Al-Subbary, A. A. 2003. Indian Ocean climate and an absolute chronology over Dansgaard/Oeschger Events 9 to 13, Science, 301, 1365–1367.

Callahan, J. E., 1972. The structure and circulation of deep water in the antarctic. Deep-Sea Res., 19, 563–575.

Caley,T., Kim, J.H., Malaizé, B., Giraudeau, J., Laepple,T., Caillon, N., Charlier, K., Rebaubier, H., Rossignol, L., Castañeda, I. S., Schouten, S., Damsté, J. S. S., 2011. High latitude obliquity forcing as a dominant forcing in the Agulhas current system. Clim.Past, 7,1285–1296.

Caley, T., S. Zaragosi1, J. Bourget, P. Martinez1, B. Malaizé, F. Eynaud, L. Rossignol, T. Garlan, and N. Ellouz-Zimmermann., 2013. Southern Hemisphere imprint for Indo-Asian summer monsoons during the last glacial period as revealed by Arabian Sea productivity records. Biogeosciences, 10, 7347–7359, doi:10.5194/bg-10-7347-2013.

Camps, P., Henry, B., Prévot, M., Faynot, L., 2001. Geomagnetic palaeosecular variation recorded in Plio-Pleistocene volcanic rocks from Possession Island (Crozet Archipelago, southern Indian Ocean). J. Geophys. Res. 106 (B2), 1961-1971.

Cefarelli, A.O., Ferrario, M.E., Almandoz, G.O., Atencio, A.G., Akselman, R., Vernet, M., 2010. Diversity of the diatom genus *Fragilariopsis* in the Argentine Sea and Antarctic waters: Morphology, distribution and abundance. Polar Biol. 33, 1463–1484.

Charles, C.D., Fairbanks, R.G., 1992. Evidence from Southern Ocean sediments for the effect of North Atlantic deep-water flux on climate. Nature 355, 416–419.

Channell, J.E.T., Xuan, C., Hodell, D.A., 2009. Stacking paleointensity and oxygen isotope data for the last 1.5 Myr (PISO-1500). Earth and Planetary Science Letters, 283, 14-23.

Chiang and Bitz 2005: Influence of high latitude ice cover on the marine Intertropical Convergence Zone. Climate Dynamics 25: 477–496DOI 10.1007/s00382-005-0040-5.

Chase, Z., Anderson, R.F., Fleisher, M.Q., Kubik, P.W., 2003. Accumulation of biogenic and lithogenic materials in the Pacific sector of the Southern Ocean during the past 40,000 years. Deep Sea Res., Part II 50, 799–832.

Clark, P.U., Dyke, A.S., Shakun, J.D., Carlson, A.E., Clark, J., Wohlfarth, B., Mitrovica, J.X., Hostetler, S.W., McCabe, A.M., 2009. The Last Glacial Maximum. Science, 325, 710-714.

Cohen, S., Willgoose, G., Hancock, G., 2013. Soil-landscape response to mid late Quaternary climate fluctuation based on numerical simulations. Quaternary Research 79, 452-457.

Comiso, J.C., 2010. Variability and trends of the global sea ice cover. In: Thomas, D.N. and Diekmann, G.S. (Eds.), Sea Ice (second edition). Blackwell, Oxford, 205-246.

Cortese, G., Abelmann, A., Gersonde R., 2007. The last five glacial-interglacial transitions: A high-resolution 450,000-year record from the subantarctic Atlantic. Paleoceanography, 22, PA4203, doi:10.1029/2007PA001457.

Cortese, G., Gersonde, R., 2007. Morphometric variability in the diatom *Fragilariopsis kerguelensis*: implications for Southern Ocean paleoceanography. Earth Planet. Sci. Lett. 257, 526–544. doi:10.1016/j.epsl.2007.03.021.

Cortese, G., Gersonde, R., Maschner, K., Medley, P., 2012. Glacial-interglacial size variability in the diatom Fragilariopsis kerguelensis: Possible iron/dust controls ?. Paleoceanography 27, PA1208, doi:10.1029/2011PA002187.

Cosford, J., Qing, H., Yuan, D., Zhang, M., Holmden, C., Patterson, W., and Hai, C., 2008. Millennial-scale variability in the Asian monsoon: evidence from oxygen isotope records from stalagmites in China, Palaeogeography, Palaeoclimatology, Palaeoecology, 266, 3–12.

Crosta, X., Romero, O., Armand, L., & Pichon, J. J. (2005a). The biogeography of major diatom taxa in Southern Ocean sediments. 2. Open ocean related species. Palaeogeography, Palaeoclimatology, Palaeoecology, 223, 66–92.

Crosta, X., Pichon, J.-J. Burkle, L.H., 1998a. Application of modern analog technique to marine Antarctic diatoms: Reconstruction of maximum sea ice extent at the Last Glacial Maximum. Paleoceanography 13, 286–297. doi:10.1029/98PA00339.

Crosta, X. and Shemesh, A., 2002, Reconciling down-core anti-correlation of diatom carbon and nitrogen isotopic ratios from the southern Ocean. *Paleoceanography*, 17(1), 1010, doi: 10.1029/2000PA000565.

Crosta, X., Sturm, A., Armand, L., Pichon, J.-J., 2004. Late Quaternary sea ice history in the Indian sector of the Southern Ocean as recorded by diatom assemblages. Mar. Micropaleontol. 50, 209–223.

Crosta, X., Romero, O., Armand, L., Pichon, J.J., 2005. The biogeography of major diatom taxa in Southern Ocean sediments: 2. Open ocean related species. Palaeogeography, Palaeoclimatology, Palaeoecology 223, 66-92.

Crosta, X. 2009. Holocene size variations in two diatom species off East Antarctica: Productivity vs environmental conditions. Deep Sea Res., Part I 56, 1983–1993.

Cunningham, W., Leventer, A., 1998. Diatom assemblages in surface sediments of the Ross Sea: relationship to present oceanographic conditions. Antarctic Science 10 (2), 134–146.

Cunningham, S.A., Alderson, S.G., King, B.A., Brandon, M.A., 2003. Transport and variability of the Antarctic Circumpolar Current in Drake Passage. Journal of Geophysical Research, 108(C5), 8084, doi:10.1029/2001JC001147.

de Vernal, A., Kageyama, M. 2006. Comparing proxies for the reconstruction of LGM sea surface conditions in the northern North Atlantic. Quaternary Science Reviews, 25, 21–22, 2820-2834.

Defelice, D. R., & Wise, S. W. 1981. Surface lithofacies, biofacies, and diatom diversity patterns as models for delineation of climatic change in the Southeast Atlantic Ocean. Marine Micropaleontology, 6, 29–70.

Denis, D., Crosta, X., Schmidt, S., Carson, D.S., Ganeshram, R.S., Renssen, H., Bout-Roumazeilles, V., Zaragosi, S., Martin, B., Cremer, M., Giraudeau, J., 2009. Holocene glacier and deep water dynamics, Adelie Land region, East Antarctica. Quaternary Science Reviews, 28, 1291-1303.

Denton, G.H., Anderson, R.F., Toggweiler, J.R., Edwards, R.L., Schaefer, J.M., Putnam, A.E., 2010. The last glacial termination. Science, 328, 1652-1656.

Deplazes, G, Andreas Lückge, Larry C. Peterson, Axel Timmermann, Yvonne Hamann1, Konrad A. Hughen, Ursula Röhl, Carlo Laj, Mark A. Cane, Daniel M. Sigman and Gerald H. Haug, 2013. Links between tropical rainfall and North Atlantic climate during the last glacial period. Nature Geosciences, DOI: 10.1038/NGEO1712.

Dezileau, L., Reyss, J. L., Lemoine, F., 2003. Late Quaternary changes in biogenic opal fluxes in the Southern Indian Ocean. Mar. Geol., 202, 143–158.

Dezileau, L., Bareille, G., Reyss, J.L., Lemoine, F., 2000. Evidence for strong sediment redistribution by bottom currents along the southeast Indian Ridge. Deep-Sea Research I 47, 1899–1936.

Diekmann, B., 2007. Sedimentary patterns in the late Quaternary Southern Ocean. Deep-Sea Research II, 54, 2350-2366.

Domack, E.W., Leventer, A., Dunbar, R., Taylor, F., Brachfeld, S., and Sjunneskog, C., and ODP Leg 178 Scientific Party, 2001. Chronology of the Palmer Deep site, Antarctic Peninsula: A Holocene palaeoenvironmental reference for the circum-Antarctic. The Holocene, 11(1), 1–9.

Dong, S., Sprintall, J., Gille, S.T., 2006. Location of the Polar Front from AMSR-E satellite sea surface temperature measurements. Journal of Physical Oceanography, 36, 2075-2089.

Downes, S. M., A. S. Budnick, J. L. Sarmiento, and R. Farneti (2011), Impacts of wind stress on the Antarctic Circumpolar Current fronts and associated subduction, Geophys. Res. Letter, 38, L11605, doi:10.1029/2011GL047668.

Dubois, N., M. Kienast, S. S. Kienast, C. Normandeau, S. E. Calvert, T. D. Herbert, and A. C. Mix, 2011: Millennial scale variations in hydrography and biogeochemistry in the eastern equatorial Pacific over the last 100 kyr. Quat. Sci. Rev., 30, 210–223.

Dutta, K., 2008. Marine 14C reservoir ages and Suess effect in the Indian Ocean. Earth Sci. India 1 (IV), 243–257.

EPICA community members, 2004. Eight glacial cycles from an Antarctic ice core. Nature, 429, 623-628.

EPICA members, 2006. One-to-one coupling of glacial climate variability in Greenland and Antarctica. Nature 444, 195-198.

Fenner, J., Schrader, H.J., Wienigk, H., 1976. Diatom phytoplankton studies in the Southern Pacific Ocean, composition and correlation to the Antarctic Convergence and its paleoecological significance. In: Hollister, C.D., Craddock, C., et al., (Eds.), Initial Reports of the Deep-Sea Drilling Project, vol. 35. U.S. Govt. Printing Office, Washington, D.C., pp. 757– 813.

Ferry, A.J., Crosta, X., Quilty, P.G., Fink, D., Howard, W., Armand, L.K., 2015, First records of winter sea-ice concentration in the southwest Pacific sector of the Southern Ocean. *Paleoceanography*, 30, 1525-1539, doi: 10.1002/2014PA002764.

Frank, M., Gersonde, R., Rutgers Van der Loe¡, M., Bohrmann, G., Nurnberg, C.C., Kubik, P.W., Suter, M., Mangini, A., 2000. Similar glacial and interglacial export bioproductivity in the Atlantic sector of the Southern ocean: Multiproxy evidence and implications for glacial atmospheric CO_2. Paleoceanography 15, 642-658.

Fryxell, G.A., Hasle, G.R., 1979. The genus *Thalassiosira*: species with internal extensions of the strutted processes. Phycologia 18 (4), 378–393.

Fryxell, G.A., Sims, P.A., Watkins, T.P., 1986. *Azpeitia* (*Bacillariophyceae*): related genera and promorphology. Am. Soc. Plant. Tax. 13, 74.

Gebregiorgis, D., Hathorne1, E.C., Giosan L., Clemens, S., Nürnberg, D., Frank, M., (2018). Southern Hemisphere forcing of South Asian monsoon precipitation over the past ~1 million Years. Nature Communications, 9:4702. Doi: 10.1038/s41467-018-07076-2.

Geibert, W., Rutgers van der Loeff, M.M., Usbeck, R., Gersonde, R., Kuhn, G., Seeberg-Elverfeldt, J., 2005. Quantifying the opal belt in the Atlantic and southeast Pacific sector of the Southern Ocean by means of 230^{Th} normalization. Global Biogeochemical Cycles 19 (GB4001), 1–13.

Gersonde, R., Zielinski, U., 2000. The reconstruction of late Quaternary Antarctic sea-ice distribution—The use of diatoms as a proxy for sea-ice, Palaeogeogr. Palaeoclimatol. Palaeoecol. 162, 263–286.

Gersonde, R., Crosta, X., Abelmann, A., Armand, L., 2005. Sea-surface temperature and sea ice distribution of the Southern Ocean at the EPILOG Last Glacial Maximum—A circum-Antarctic view based on siliceous microfossil records. Quat. Sci. Rev. 24, 869–896.

Gille, S.T., 1994. Mean sea surface height of the Antarctic Circumpolar Current from Geosat data: method and application. Journal of Geophysical Research, 99, 18255-18273.

Budd, W. F. 1975. Antarctic Sea-Ice Variations from Satellite Sensing in Relation to Climate. Journal of Glaciology, 15, 73, 417-427.

Giret, P.A., Weis, D., Zhou, X., Cottin, J.-Y., Tourpin, S., 2003. Les Îes Crozet. Géologues 137, 15-23.

Guiot, J. 1990. Methodology of the last climatic cycle reconstructions in France from pollen data. Palaeogeography, Palaeoclimatology, Palaeoecology, 80, 49–69.

Guiot, J. & de Vernal, A. 2011. Is spatial autocorrelation introducing biases in the apparent accuracy of paleoclimatic reconstructions? Quaternary Science Reviews 30, 1965–1972.

Hall, B.L., 2009. Holocene glacial history of Antarctica and the sub-Antarctic islands. Quat. Sci. Rev. 28, 2213-2230.

Hasle, G. R. (1969). An analysis of the phytoplancton of the Pacific Southern Ocean: Abundance, composition, and distribution during the Brategg Expedition, 1947–1948, 168. Oslo, Norway: Universitetsforlaget.

Hasle, G.R., 1965. Nitzschia and Fragilariopsis species studied in the light and electron microscope: III. The genus Fragilariopsis. Skrifter utgitt av det Norske Videnskaps-Akademi, Oslo,18, 1– 45.

Hasle, G.R., Syvertsen, E.E., 1996. Marine Diatoms. In: Tomas, C.R. (Ed), Identifying Marine Phytoplankton, Academic Press, London, pp. 5–385.

Hays, J.D., Imbrie, J., Shackleton, N.J., 1976. Variations in the earth's orbit: pacemaker of the ice ages. Science, 194, 1121-1132.

Hein, A.S., Hulton, N.R.J., Dunai, T.J., Sugden, D.E., Kaplan, M.R., Xu, S., 2010. The chronology of the Last Glacial Maximum and deglacial events in central Argentine Patagonia. Quaternary Science Reviews, 29, 1212-1227.

Hillenbrand, C.-D., Smith, J.A., Kuhn, G., Esper, O., Gersonde, R., Larter, R.D., Maher, B., Moreton, S.G., Shimmield, T.M., Korte, M., 2009. Age assignment of a diatomaceous ooze deposited in the western Amundsen Sea Embayment after the Last Glacial Maximum. Journal of Quaternary Science, ISSN 0267-8179.

Hillenbrand, C.-D. and Cortese, G., 2006. Polar stratification: A critical view from the Southern Ocean. Palaeogeography, Palaeoclimatology, Palaeoecology 242, 240-252.

Horner, R., 1984. Do ice algae produce the spring phytoplankton bloom in seasonally ice-covered waters? In: Koeltz, O. (Ed.), Proceedings of the 7th Diatom Symposium, Philadelphia, 1982. Koenigstein, pp. 401-409

Hustedt, F., 1930. Die Kieselalgen Deutschlands, O¨ sterreichs und der Schweiz. In: Rabenhorst, L. (Ed.), Kryptogamen-Flora Deutschlands. O¨ sterreichs und der Schweiz, pp. 1– 920.

Hustedt, F., 1958. Diatomeen aus der Antarktis und dem Sqdatlantik. Reprinted from bDeutsche Antarktishe Expedition 1938/1939Q Band II, Geographisch-kartographische Anstalt bMundusQ. Hamburg. 191 pp. pl. 3–13.

Ivanochko, T. S., Ganeshrama, R. S., Brummer, G-J. B., Ganssen, G., Jung, S. J. A., Moreton, S. G., and Kroon, D., 2005. Variations in tropical convection as an amplifier of global climate change at the millennial scale, Earth Planet. Sci. Lett., 235, 302–314.

Jaccard S. L., Hayes C. T., Martínez-García A., Hodell D. A., Anderson R. F., Sigman D. M., Haug G. H., 2013. Two Modes of Change in Southern Ocean Productivity over the Past Million Years. Science 339, 1419-1423. (doi:10.1126/science.1227545).

Jansen, et al., 2007. Chapter 6, Paleoclimate, Intergovernmental Panel on Climate Change (IPCC) report 2007, in Climate Change 2007 – The Physical Science Basis. Cambridge University Press, Cambridge. 433-497.

Jenkins, D.G., 1974. Initiation of the proto circum-Antarctic current. Nature 252, 371 – 373

Johansen, J.R., Fryxell, G.A., 1985. The genus *Thalassiosira* (*Bacillariophyceae*): studies on species occurring south of the Antarctic Convergence. Phycologia 24 (2), 155– 179.

Jouzel et al., 2007. Orbital and Millennial Antarctic Climate Variability over the Past 8,00,000 years. Science, 317, No. 5839, pp.793-797.

Kaczmarska, I., Barbrick, N.E., Ehrman, J.M., Cant, G.P., 1993. Eucampia index as an indicator of the Late Pleistocene oscillations of the winter sea-ice extent at the ODP Leg 119 Site 745B at the Kerguelen Plateau. Hydrobiologia, 269/270, 103-112.

Koutavas, A., and J. P. Sachs, 2008: Northern timing of deglaciation in the eastern equatorial Pacific from alkenone paleothermometry. Paleoceanography, 23, PA4205, doi:10.1029/2008PA001593.

Kohfeld, K.E., Le Quere, C., Harrison, S.P., Anderson, R.F., 2005. Role of marine biology in glacial-interglacial CO2 cycles. Science, 308, 74-78.

Kohfeld, K.E., Graham, R.M., de Boer, A.M., Sime, L.C., Wolff, E.W., Le Quéré, C., Bopp, L. 2013. Southern Hemisphere westerly wind changes during the Last Glacial Maximum: Paleo-data synthesis, Quat. Sci. Rev. 68, 76–95.

Kumar, N., Anderson, R.F., Mortlock, R.A., Froelich, P.N. Kubik, P., Diirich-Hannen, B., Suter, M., 1995. Increased biological productivity and export production in the glacial Southern Ocean, Nature 378, 675–680.

Lamy F *et al*. 2014 Increased dust deposition in the Pacific Southern Ocean during glacial periods. *Science* **343**, 403–407. doi:10.1126/science.1245424.

Lawver, L.A. and Gahagan, L.M., 2003. Evolution of Cenozoic seaways in the circum-Antarctic region. Palaeogeography, Palaeoclimatology, Palaeoecology, 198, 11-38.

Lea, D. W., D. K. Pak, L. C. Peterson, and K. A. Hughen, 2003: Synchronicity of tropical and high-latitude Atlantic temperatures over the last glacial termination. Science, 301, 1361–1364.

Lebouvier, M., Frenot, Y., 2007. Conservation and management in the French sub-Antarctic islands and surrounding seas. Pap. Proc. R. Soc. Tasmania. 141 (1), 23-28.

Lisiecki, L.E. and Raymo, M.E., 2005. A Pliocene-Pleistocene stack of 57 globally distributed benthic _18O records. Paleoceanography, 20, PA1003, doi: 10.1029/2004PA001071.

Lowe, JJ, Rasmussen SO, Bjo¨rck S, Hoek WZ, Steffensen JP, Walker MJC, Yu Z. the INTIMATE group. 2008b. Precise dating and correlation of events in the North Atlantic region during the Last Termination: a revised protocol recommended by the INTIMATE group. Quaternary Science Reviews 27: 6–17.

Lund, S., Stoner, J.S., Channell, J.E.T., Acton, G., 2006. A summary of Brunhes paleomagnetic variability recorded in Ocean Drilling Program cores. Physics of the Earth and Planetary Interiors, 156, 194-204.

Mackensen, A. 2004. Changing Southern Ocean palaeocirculation and effects on global climate. Antarctic Science, 16, 369-386.

Macri, P., Sagnotti, L., Lucchi, R.G., Rebesco, M., 2006. A stacked record of relative geomagnetic paleointensity for the past 270 kyr from the western continental rise of the Antarctic Peninsula. Earth and Planetary Science Letters, 252, 162-179.

Maher, B. A., M. Prospero, D. Mackie, D. Gaiero, P. P. Hesse, Y. Balkanski. 2010. Global connections between aeolian dust, climate and ocean biogeochemistry at the present day and at the last glacial maximum. Earth-Science Reviews, 99, 1–2, 61-97.

Mann, D.G., 1993. Patterns of sexual reproduction in diatoms. Hydrobiology 269-270, 11-20.

Manoj, M. C., Thamban, M., Basavaiah, N., Mohan, R., 2012. Evidence for climatic and oceanographic controls on terrigenous sediment supply to the Indian Ocean sector of the Southern Ocean over the past 63,000 years. Geo Mar. Lett. 32(3), 251. doi:10.1007/s00367-011-0267-6.

Manoj, M.C., 2014. Geochemical Studies on Late Quaternary Sediments from the Indian Sector of Southern Ocean and its Palaeoenvironmental Implications (Ph.D. dissertation). Goa University, India.

Manoj, M. C., Thamban, M., 2015. Shifting frontal regimes and its influence on bioproductivity variaiton during the Late Quaternary in the Indian sector of Southern Ocean. Deep Sea Res., Part II. doi:10.1016/j.dsr2.2015.03.011.

Margo members, 2009. Constraints on the magnitude and patterns of ocean cooling at the Last Glacial Maximum. Nature Geoscience 2, 127-132.

Martinez-Garcia, A., A. Rosell-Mele, S. L. Jaccard, W. Geibert, D. M. Sigman, and G. H. Haug (2011), Southern Ocean dust-climate coupling over the past four million years, Nature, 476, 312–315.

Martínez-Garcia, A., Rosell-Mele, A., Geibert, W., Gersonde, R., Masqué, P., Gaspari, V., Barbante, C., 2009. Links between iron supply, marine productivity, sea surface temperature, and CO2 over the last 1.1 Ma. Paleoceanography, 24, p. PA1207, 10.1029/2008PA001657.

Martinson, D.G., Pisias, N.G., Hays, J.D., Imbrie, J., Moore Jr., T.C., Shackleton, N.J., 1987. Age dating and the orbital theory of the ice ages: development of a high-resolution 0 to 300,000-year chronostratigraphy. Quaternary Research, 27, 1-29.

Martinson, D. G., 2012. Antarctic circumpolar current's role in the Antarctic ice system: An overview, Palaeogeography, Palaeoclimatology, Palaeoecology, 335-336, 71–74.

Mayewski, P., Rohling, E., Stager, C., Karlen, W., Maasch, K.A., Meeker, L.D., Meyerson, E.A., Gasse, F., van Kreveld, S., Holmgren, K., Lee-Thorp, J., Rosqvist, G., Rack, F., Staubwasser, M., Schneider, R.R., Steig, E.J.,2004. Holocene climate variability. Quaternary Research 62, 243-255.

McManus, J.F., Francois, R., Gherardi, J.-M., Keigwin, L.D., Brown-Leger, S., 2004. Collapse and rapid resumption of Atlantic meridional circulation linked to deglacial climate change. Nature, 428, 834-837.

McDougall, I., Verwoerd, W., Chevallier, L., 2001. K-Ar geochronology of Marion Island, southern Ocean. Geol. Mag. 138, 1-17.

McCoy, F.W., 1991. Southern Ocean sediments: circum-Antarctic to 301S. In: Hayes, D.E. (Ed.), Marine Geological and Geophysical Atlas of the Circum-Antarctic to 301S. Antarctic Research Series, vol. 54. American Geophysical Union, Washington, DC, pp. 37–46.

Moore, J.K., Abbott, M.R., Richman, J.G., 1999. Location and dynamics of the Antarctic Polar Front from satellite sea surface temperature data. Journal of Geophysical Research, 104(C2), 3059-3073.

Moore, J.K., Abbott, M.R. and Richman, J.G., 1997. Variability in the location of the Antarctic Polar Front (90_-20_W) from satellite sea surface temperature data. Journal of Geophysical Research, 102(C13), 27825-27833.

Moore, J.K., Abott, M. R., Richman, J. G., Nelson, D. M., 2000. The Southern Ocean at the last glacial maximum: A strong sink for atmospheric carbon dioxide. Global biogeochemical cycles, 14, 1, 455-475.

Nair, A., Mohan, R., Manoj, M.C., Thamban, M., 2015. Glacial-interglacial variability in diatom abundance and valve size: Implications for Southern Ocean paleoceanography. Paleoceanography 30. doi:10.1002/2014PA002680.

Neil, H. L., L. Carter, and M. Y. Morris (2004), Thermal isolation of Campbell Plateau, New Zealand, by the Antarctic Circumpolar Current over the past 130 kyr, Paleoceanography, 19, PA4008, doi:10.1029/2003PA000975.

NGRIP members, 2004: High-resolution record of Northern Hemisphere climate extending into the last interglacial period, Nature, 431, 147–151.

Olbers, D., Borowski, D., Voelker, C., Woelff, J.-O., 2004. The dynaical balance, transport and circulation of the Antarctic Circumpolar Current. Antarctic Science, 16(4), 439-470.

Orsi, A.H., Whitworth III, T., Nowlin Jr. W.D., 1995. On the meridional extent and fronts of the Antarctic Circumpolar Current. Deep Sea Res.,Part I 45, 641–673.

Quilty, P.G., 2007. Origin and evolution of the sub-Antarctic islands: the foundation. Pap. Proc. R. Soc. Tasmania. 141 (1), 35-58.

Park, Y.H., Gamberoni, L., Charriaud, E., 1993. Frontal structure, water masses and circulation in the Crozet Basin. J. Geophys. Res. 98 12, 361–12,385.

Peterson, L. C., G. H. Haug, K. A. Hughen, and U. Röhl, 2000: Rapid changes in the hydrologic cycle of the tropical Atlantic during the last glacial. *Science*, **290**, 1947–1951, doi:10.1126/science.290.5498.1947.

Peeters, F.J.C., Acheson, R., Brummer, G.-J.A., de Ruijter, W.P.M., Schneider, R.R., Ganssen, G.M., Ufkes, E., Kroon, D., 2004. Vigorous exchange between the Indian and Atlantic oceans at the end of the past five glacial periods. Nature 430, 661–665.

Pollard, R.T., Read, J.F., 2001. Circulation pathways and transports of the Southern Ocean in the vicinity of the Southwest Indian Ridge. Journal of Geophysical Research 106, 2881–2898.

Pollard, R.T., Lucas, M.I., Read, J.F., 2002. Physical controls on biogeochemical zonation in the Southern Ocean, Deep Sea Res., Part II 49, 3289–3305.

Pollard, R.T., Venables, H.J., Read, J.F., Allen, J.T., 2007. Large-scale circulation around the Crozet Plateau controls an annual phytoplankton bloom in the Crozet Basin. Deep Sea Res., Part II 54, 1915–1929.

Pondaven, P., Ragueneau, T., Tre´guer, P., Hauvespre, A., Dezileau, L., Reyss, J.L., 2000. Resolving the 'opal paradox' in the Southern Ocean. Nature 405, 168–172.

Prell, W. L. (1985). The stability of low-latitude sea-surface temperatures: An evaluation of the CLIMAP reconstruction with emphasis on the positive SSTanomalies. Report TR 025, US Department of Energy Washington D.C., pp. 1–60.

Pugh, R.S., McCave, I.N., Hillenbrand, C.-D., Kuhn, G., 2009. Circum-Antarctic age modeling of Quaternary marine cores under the Antarctic Circumpolar Current: Ice-core dust-magnetic correlation. Earth and Planetary Science Letters, 284, 113-123.

Pudsey, C.J., Howe, J.A., 1998. Quaternary history of the Antarctic Circumpolar Current: evidence from the Scotia Sea. Marine Geology 148, 83–112.

Ragueneau, O., Tre´guer, P., Leynaert, A., Anderson, R. F., Brezinski, M. A., DeMaster, D. J., Dugdale, R. C., Dymont, J., Fisher, G., Franc- ois, R., Heinze, C., Maier-Reimer, E., Martin- Je´ze´quel, V., Nelson, D. M., & Que´guiner, B. (2000). A review of the Si cycle in the modern ocean: Recent progress and missing gaps in the application of biogenic opal as a paleoproductivity proxy. Global and Planetary Change, 26, 317–365.

Rintoul, S. R., Hughes, C., Olbers, D., 2001. The Antarctic circumpolar current system, in Ocean, Ice and Atmosphere. In: Siedler, G., Church, J,. Gould, J. (Eds), Interactions at the Antarctic Continental Margin, Academic Press, San Diego, London, pp. 151–171.

Rohling, E. J., Mayewski, P. A., and Challenor, P., 2003. On the timing and mechanism of millennial-scale climate variability during the last glacial cycle, Clim. Dynam., 20, 257–267.

Rohling, E. J., Liu, Q. S., Roberts, A. P., Stanford, J. D., Rasmussen, S. O., Langen, P. L., and Siddall, M., 2009. Controls on the East Asian monsoon during the last glacial cycle, based on comparison between Hulu Cave and polar ice-core records, Quat. Sci. Rev., 28, 3291–3302. doi:10.1016/j.quascirev.2009.09.007, 2009.

Romero, O., Armand, L. K., Crosta, X., & Pichon, J. J. (2005). The biogeography of major diatom taxa in Southern Ocean sediments: 3. Tropical/subtropical species. Palaeogeography, Palaeoclimatology, Palaeoecology, 223, 49–65.

Round, F.E., Crawford, R.M., Mann, D.G. (Eds.), 1990. The Diatoms: Biology and Morphology of the Genera. Cambridge University Press, Cambridge, p. 747.

Sabine, C. L., Richard A. Feely, Nicolas Gruber, Robert M. Key, Kitack Lee, John L. Bullister, Rik Wanninkhof, C. S. Wong, Douglas W. R. Wallace, Bronte Tilbrook, Frank J. Millero, Tsung-Hung Peng, Alexander Kozyr, Tsueno Ono, Aida F. Rios, 2004. The Oceanic Sink for Anthropogenic CO_2. Science, 305, 5682, 367-371. DOI: 10.1126/science.1097403.

Sancetta, C. (1992). Comparison of phytoplankton in sediment trap series and surface sediments along a productivity gradient. Paleoceanography, 7(2), 183–194.

Schlu¨ ter, M., Rutgers van der Loeff, M.M., Holby, O., Kuhn, G., 1998. Silica cycle in surface sediments of the South Atlantic. Deep-Sea Research I 45, 1085–1109.

Schrader, H. J., Gersonde, R., 1978. Diatoms and silicoflagellates. In: Zachariasse, W.J., et al. (Eds.), Micropaleontological Counting Methods and Techniques: An Exerciseon an Eight Metres Section of the Lower Pliocene of Capo Rossello, Sicily. Utrecht Micropaleontol. Bull. 17, Utrecht, Netherlands, pp. 129–176.

Schmieder, F., 2004. Magnetic signals in Plio-Pleistocene sediments of the South Atlantic: Chronostratigraphic usability and paleoceanographic implications; In: The South Atlantic in the late Quaternary: Reconstruction of material budgets and current systems (eds) Wefer, G., Mulitza, S. and Ratmeyer, V. (Springer-Verlag: Berlin), pp. 261–277.

Scher, H.D. and Martin, E.E., 2006. Timing and climatic consequences of the opening of Drake Passage. Science, 312, 428-430.

Schulz, H., von Rad, U., Erlenkeuser, H. 1998. Correlation between Arabian Sea and Greenland climate oscillations of the past 110 000 years, Nature, 393, 54–57.

Semina, H. J. 2003. SEM-studied diatoms of different regions of the World Ocean. Iconographia Diatomologica, 10, 1–362.

Simonsen, R. (1974). The diatom plankton of the Indian Ocean Expedition of R/V Meteor 1964/1965. Meteor Forschergeb Reihe D, 19, 1–107.

Scott, F.P., Thomas, D.P., 2005. Diatoms. In: F.P. Scott., Marchant, H.J. (Eds.), Antarctic Marine Protists, Aust. Biol. Resour. Study and Aust. Antarct. Div., Hobart, pp. 13–201.

Shukla, S.K., Crosta, X., Cortese, G., Nayak, G.N., 2013. Climate mediated size variability of diatom *Fragilariopsis kerguelensis* in the Southern Ocean. Quat. Sci. Rev. 69, 49–58. doi:10.1016/j.quascirev.2013.03.005.

Shukla, S.K., Crespin, J. & Crosta, X. 2016. Thalassiosira lentiginosa size variation and associated biogenic silica burial in the Southern Ocean over the last 42 kyrs. Marine Micropalaeontology, 127, 10.1016/j.marmicro.2016.07.006.

Sigman, D. M., and E. A. Boyle (2000), Glacial/interglacial variation in atmospheric carbon dioxide, Nature, 40, 859–869.

Sigman, D.M., Jaccard, S.L., Haug, G.H., 2004. Polar ocean stratification in a cold climate. Nature, 428, 59-63.

Sigman, D.M., Hain, M.P., Haug, G.H., 2010. The polar ocean and glacial cycles in atmospheric CO2 concentration. Nature, 466, 47-55.

Sikes, E. L., Samson, C. R., Guilderson, T. P., Howard, W. R., 2000. Old radiocarbon ages in the southwest Pacific Ocean during the last glacial period and deglaciation. Nature, 405, 555-559.

Simon, M.H., Arthur, K.L., Hall, I.R., Peeters, F.J.C., Loveday, B.R., Barker, S., Ziegler, M., Zahn, R., 2013. Millennial-scale Agulhas Current variability and its implications for salt-leakage through the Indian-Atlantic Ocean gateway. Earth Planet. Sci. Lett. 383, 101–112.

Skinner, L.C., Fallon, S., Waelbroeck, C., Michel, E., Barker, S., 2010. Ventilation of the deep Southern Ocean and deglacial CO2 rise. Science, 328, 1147-1151.

Smetacek, V., 1985. Role of sinking in diatom life-history cycles: ecological, evolutionary and geological significance. Marine Biology, 84, 239-251.

Sokolov, S., Rintoul, S.R., 2007. On the relationship between fronts of the Antarctic Circumpolar Current and surface chlorophyll concentrations in the Southern Ocean, J. Geophys. Res. 112(C7), 1–17. doi:10.1029/2006JC004072.

Sokolov, S., and S. R. Rintoul, 2009a, Circumpolar structure and distribution of the Antarctic Circumpolar Current fronts: 1. Mean circumpolar paths, J. Geophys. Res., 114, C11018, doi:10.1029/2008JC005108.

Sokolov, S., and S. R. Rintoul, 2009b, Circumpolar structure and distribution of the Antarctic Circumpolar Current fronts: 2. Variability and relationship to sea surface height, J. Geophys. Res., 114, C11019, doi:10.1029/2008JC005248.

Stephens, B.B. and Keeling, R.F., 2000. The influence of Antarctic sea ice on glacial-interglacial CO2 variations. Nature, 404, 171-174.

Stoner, J.S., Lay, C., Channell, J.E.T., Kissel, C., 2002. South Atlantic and North Atlantic geomagnetic paleointensity stacks (0-80 ka): implications for inter-hemispheric correlation. Quaternary Science Reviews, 21, 1141-1151.

Stouffer, RJ, Yin J, Gregory JM, Dixon KW, Spelman MJ, et al. 2006. Investigating the causes of the response of the thermohaline circulation to past and future climate changes. J. Clim. 19:698–722

Stuiver, M., Reimer, P.J., Reimer, R.W., 2005. CALIB 6.0 [Program and documentation]. [Available at http://www.calib.qub.ac.uk/.]

Sumner, P.D., Meiklejohn, K.I., Boelhouwers, J.C., Hedding, D.W., 2004. Climate change melts Marion Island snow and ice. S. Afr. J. Sci. 100, 395-398.

Tierney J, E., James M. Russell, Yongsong Huang, Jaap S. Sinninghe Damsté, Ellen C. Hopmans, Andrew S. Cohen, 2008. Northern Hemisphere Controls on Tropical Southeast African Climate During the Past 60,000 Years. Science VOL 322, 252-254.

Thamban, M., Naik, S.S., Mohan, R., Rajakumar, A., Basavaiah, N., D'Souza, W., Kerkar, S., Subramaniam, M.M., Sudhakar, M., Pandey, P.C., 2005. Changes in the source and transport mechanism of terrigenous input to the Indian Ocean sector of Southern Ocean

during the late Quaternary and its palaeoceanographic implications. J. Earth. Syst. Sci. 114(5) 443–452.

Tomas, R. A., P. J. Webster, The role of inertial instability in determining the location and strength of near-equatorial convection. Q. J. R. Meteorol. Soc. 123, 1145 (1997). doi:10.1002/qj.49712354202

Toggweiler, J. R., 1994 and B. Samuels, 1993: Is the magnitude of the deep outflow from the Atlantic Ocean actually governed by Southern Hemisphere winds? The Global Carbon Cycle, M. Heimann, Ed., Springer, 303–331.

Treguer, P., Jacques, G., 1992. Dynamics of nutrients and phytoplankton, and fluxes of carbon, nitrogen and silicon in the Antarctic Ocean. Polar Biol. 12, 149–162.

van Beek, P., Reyss, J-L., Paterne, M., Gersonde, R., van der Loeff, M.R., Kuhn, G., 2002. 226Ra in barite: Absolute dating of Holocene Southern Ocean sediments and reconstruction of sea-surface reservoir ages. Geology, 30(8), 731–734.

Villareal, T.A., Fryxell, G.A., 1983. The Genus Actinocyclus (Bacillariophyceae): frustule morphology of A. sagittulus sp. nov. and two related species. Journal of Phycology 19, 266– 452.

Wang, Y. J., H. Cheng, R. L. Edwards, Z. S. An, J. Y. Wu, C. C. Shen, and J. A. Dorale, 2001: A high-resolution absolute-dated late Pleistocene monsoon record from Hulu Cave, China. Science, 294, 2345–2348, doi:10.1126/science.1064618.

Wang, Y. J., and Coauthors, 2008: Millennial- and orbital-scale changes in the East Asian monsoon over the past 224,000 years. Nature, 451, 1090–1093.

Webster, P., in The Hadley Circulation: Present, Past and Future, H. F. Diaz, R. S. Bradley, Eds. (Kluwer Academic Publishers, 2005), pp. 9–60.

Whitworth, III, T. and Peterson, R.G., 1985. Volume transport of the Antarctic Circumpolar Current from bottom pressure measurements. Journal of Physical Oceanography, 15, 810–816.

Yokoyama, Y., Lambeck, K., de Dekker, P., Johnston, P., Fifield, K., 2000. Timing for the maximum of the Last Glacial constrained by lowest sea-level observations. Nature 406, 713-716.

You, Y.Z., 2000. Implications of the deep circulation and ventilation of the Indian Ocean on the renewal mechanism of North Atlantic Deep Water. J. Geophys. Res. 105, 23895–23926.

Yuan D, Hai Cheng, R. Lawrence Edwards,Carolyn A. Dykoski, Megan J. Kelly, Meiliang Zhang, Jiaming Qing, Yushi Lin, Yongjin Wang, Jiangyin Wu, Jeffery A. Dorale, Zhisheng An, Yanjun Cai, 2004. Timing, Duration, and Transitions of the Last Interglacial Asian Monsoon. Science, 304, 23, 575-578.

Zachos, J., Pagani, M., Sloan, L., et al., 2001.Trends, rhythms, and aberrations in global climate 65 Ma to Present. Science, 292, 686-693.

Zielinski, U. 1993. Quantitative estimation of palaeoenvironmental parameters of the Antarctic Surface Water in the Late Quaternary using transfer functions with diatoms.

Ph.D. thesis, Alfred Wegener Institute for Polar and Marine Research, Bremerhaven, Germany, p. 171.

Zielinski, U., Gersonde, R., 1997. Diatoms distribution in Southern Ocean surface sediments (Atlantic sector): Implications for paleoenvironmental reconstructions. Palaeogeogr. Palaeoclimatol. Palaeoecol. 129, 213–250.

Zielinski, U. and Gersonde, R., 2002. Plio-Pleistocene diatom biostratigraphy from ODP Leg 177, Atlantic sector of the Southern Ocean. Marine Micropaleontology, 45, 225-268.

Zielinski, U., Bianchi, C., Gersonde, R., Kunz-Pirrung, M., 2002. Last occurrence datums of the diatoms *Rouxia leventerae* and *Rouxia constricta*: indicators for marine isotope stages 6 and 8 in Southern Ocean sediments. Marine Micropaleontology, 46, 127-137.

Publication